Performance of MIMO CDMA in Impulsive Channels

Hasan Saed Abu Hilal

Submitted to the
Institute of Graduate Studies and Research
in partial fulfillment of the requirements for the degree of

Doctor of Philosophy
in
Electrical and Electronic Engineering

Eastern Mediterranean University
July 2012
Gazimağusa, North Cyprus

Approval of the Institute of Graduate Studies and Research

Prof. Dr. Elvan Yılmaz
Director

I certify that this thesis satisfies the requirements as a thesis for the degree of Doctor of Philosophy in Electrical and Electronic Engineering

Assoc. Prof. Dr. Aykut Hocanın
Chair, Electrical and Electronic Engineering

We certify that we have read this thesis and that in our opinion it is fully adequate, in scope and quality as a thesis of the degree of Doctor of Philosophy in Electrical and Electronic Engineering

Assoc. Prof. Dr. Hüseyin Bilgekul
Cosupervisor

Assoc. Prof. Dr. Aykut Hocanın
Supervisor

Examining Committee

1. Prof. Dr. Hakan A. Çırpan
2. Prof. Dr. Hasan Amca
3. Assoc. Prof. Dr. Aykut Hocanın
4. Assoc. Prof. Dr. Erhan A. İnce
5. Assoc. Prof. Dr. Hüseyin Bilgekul

ABSTRACT

In this thesis, multiple-input and multiple-output (MIMO) communication systems, in code division multiple access (CDMA) settings, and vertical-bell layered space time (VBLAST) algorithms are investigated. The performance of linear CDMA detectors, operating in an environment with interference due to non-Gaussian noise and time mismatch is considered. The robust successive interference cancellation (RSIC) and robust space time decorrelating detectors (RSTDD) are employed to detect the signals received by multi receiving antennas having time mismatches. The performance of the detectors in practical situations such as incomplete channel state information, correlated antennas, and impulsive noise is investigated. The results show that RSIC and RDD have a good performance in adverse conditions.

The performance of the DD in MIMO CDMA system under two different impulsive noise models is examined. A robust detection technique is proposed to overcome the impulsive effect on the system. Maximal ratio combining (MRC) and post detection combining (PDC) are used to achieve diversity reception. We show that the proposed RDD outperforms the linear decorrelating detector (DD) consistently for the ideal and power imbalanced cases.

Furthermore, we analyzed and derived the probability of bit error (P_b) expression of a successive interference cancellation (SIC) system for MRC and PDC schemes. The performance bounds were also derived and depicted for identically independent distributed variances at the receiving ends. It is found that the MRCSIC has higher

performance for equal variances at the receiving antennas. On the other hand, the PDCSIC performs better when the variances are i.i.d.

Keywords: CDMA, MIMO CDMA, diversity, impulsive noise, robust detection, VBLAST, SIC, channel estimation, time mismatch, multiuser detection.

ÖZ

Bu tezde, çok-girişli-çok-çıkışlı (MIMO) iletişim sistemlerinin Kod Bölüşümlü Çoklu Erişim (CDMA) ortamında başarımı incelenmiştir. Telsiz iletişim sistemlerinde Gauss dağılımı ile modellenemeyen fiziksel etkenler dürtün gürültüye yol açmakta ve çoklu iletişim sistemlerinin başarımını etkilemektedir.
Çoklu erişim ve VBLAST algoritmaları konularında özgün öneriler yapılmıştır. Gürbüz ardışıl girişim azaltıcı (RSIC) ve gürbüz zaman-uzay özilinti gideren sezici (RSTDD) kullanılarak çok verici ve alıcı anten sistemlerindeki başarım araştırılmış ve yeni seziciler önerilmiştir. Önerilen sezicilerin kestirim hatalarının bulunduğu durumlarda ve diğer olumsuz koşullardaki başarımı incelenmiştir.

Kanal kestiriminin doğrusal çoklu ilintisizleştirici seziciye etkisi gösterilmiş ve gürbüz alıcı önerisi yapılmıştır. Gürbüz alıcı kestirim hatalarını kanal matrisini değiştirerek ve zamanlama hatalarını da yayma matrisini düzenleyerek azaltmaktadır. Dürtün gürültünün etkileri ise bir doğrusalsızlık işlemcisi ile giderilmektedir. Gürbüz sezici, bit hata oranını düşürmekte ve sistem sığasını artırmaktadır.

Dürtün gürültünün VBLAST algoritmasına etkisi, Middleton Class A gürültü modeli altında benzetimler ile incelenmiş ve kanal kestirim hatalarının başarıma olumsuz etki yaptığı gösterilmiştir. Farklı birleştirme tekniklerinin MIMO CDMA sistemlerine etkisi incelenmiş ve analitik sonuçlar sunulmuştur. Alınan sinyalin güç dengesizliğinin olduğu durumda gürbüz sezicinin hangi oranda etkilendiği de incelenmiştir. En büyük oranı seçen birleştirme (MRCSIC) tekniği kullanıldığında eşit değişintili işaretler için

yüksek başarım elde edilmektedir. İşaret değişintilerinin eşit dağılıma sahip olduğu durumda ise sezim sonrası alıcının (PDCSIC) daha başarılı olduğu gözlemlenmiştir.

Anahtar Kelimeler: CDMA, VBLAST, ilintisizleştirici sezici, ardışıl girişim azaltma, kanal kestirimi, dürtün gürültü.

ACKNOWLEDGMENTS

First and foremost, I would like to thank my supervisor Assoc. Prof. Dr. Aykut Hocanın, for his warm encouragement, valuable guidance, constant support, and the advice and care he has imparted on me during this research. I would like to express my gratitude in saying ”for the world you are one person, and for one person you are the world, and that person is me”. I am extremely grateful to my co-supervisor Assoc. Prof. Dr. Hüseyin Bilgekul for his advice and positive criticism on both technical and non-technical matters. I cannot begin to thank the countless people that have influenced my life and education. I apologize in advance to all the people I forget to mention, but I want to mention Dr. Mohammad Salman for his help.

I would like to express my deepest gratitude to my family, Mohammad and Yaseen for giving me the opportunity to build a successful career. Finally, I wish also to thank staffs and colleagues at the EEE department.

DEDICATION

Dedicated to my family

TABLE OF CONTENTS

LIST OF FIGURES

LIST OF SYMBOLS AND ABBREVIATIONS

A	Amplitude matrix
B_D	Doppler spread
B_c	Coherence bandwidth
C	Fading coefficients Matrix for MIMO CDMA
f_c	Carrier frequency
f_d	Doppler frequency shift
f_m	Maximum Doppler frequency shift
H	Fading coefficients Matrix for MIMO V-BLAST
S	Spreading code matrix
n	Noise vector
K	Number of users in one CDMA cell
N	Spreading factor
M	Number of bits in one frame
N_R	Number of receiving antennas
N_T	Number of transmitting antennas
R	Correlation matrix
r	Received data vector
T_c	Chip duration
T_s	Symbol duration
w	Tap weights vector

X	Poisson impulsive power ratio index
Z	Poisson impulsive index
ϵ	Impulsive noise frequency
κ	Impulsive noise strength
μ	Threshold value
σ^2	Variance
σ_τ	rms delay spread
ρ	Cross-correlation value
τ	Time delay
$\overline{\tau}$	Mean excess delay

AWGN	Additive White Gaussian Noise
BER	Bit Error Rate
BPSK	Binary Phase Shift Keying
CDMA	Code Division Multiple Access
CLT	Central Limit Theorem
DS-CDMA	Direct Sequence Code Division Multiple Access
DD	Decorrelating Detector
FDMA	Frequency Division Multiple Access
GSM	Global System for Mobile Communication
ISI	Inter-Symbol Interference
LMS	Least Mean Square
LOS	Line-of-Sight

MAI	Multiple Access Interference
MAP	Maximum A posteriori Probability
MC-CDMA	Multicarrier Code Division Multiple Access
ML	Maximum Likelihood
MLSE	Maximum Likelihood Sequence Estimation
MRC	Maximal Ratio Combining
MSE	Mean Square Error
NLOS	Non-Line-of-Sight
PDC	Post Detection Combining
pdf	probability density function
pmf	probability mass function
QPSK	Quadrature Phase Shift Keying
RSIC	Robust Successive Interference Cancellation
RSTDD	Robust Space-Time Decorrelating Detector
SIC	Successive Interference Cancellation
SINR	Signal to Interference and Noise Ratio
SNR	Signal to Noise Ratio
SS	Spread Spectrum
STDD	Space-Time Decorrelating Detector
STC	Space-Time Coding
UMTS	Universal Mobile Telecommunication System
V-BLAST	Vertical-Bell Layered Space Time
W-CDMA	Wideband Code Division Multiple Access

Chapter 1

INTRODUCTION

1.1. Introduction

In the past, network operators offered primarily telephony (voice) and occasionally pager services based on 2G mobile networks. However, consumer demands for faster communications downsized the second generation (2G), and replaced it with the third generation (3G) communication system. Now it is the year 2012 and the mobile telecom sector has been introduced to the MIMO communication systems. The technical recommendations by the 3GPP to ITU-T in the fall 2009, was to use long term evolution (LTE) state-of-the-art IMT-leading-edge standard.

Technology has also developed from making bulky and cumbersome products to small and elegant products. Therefore, the future customers will ask for additional services and hardware features, such as email, fax, local area network, internet access, video services, and touch screen interface. A short list of probable features include:

1. Cost effective high speed hardware on hand.
2. Wide range of accessibility.
3. Applications-rich user devices.

Therefore, it is expected to develop equipment and provide a network access for these future demands. However, this is a high cost investment and network operators need to be certain of some return on their investment.

The advance mobile phone system (AMPS) was the first mobile phone network and was based on analog radio transmission systems. The 2G global system for mobile (GSM) system was selected by the market to handle increased traffic inside the network, and was initiated in the nineties. This traffic was the main reason for dropped calls and was increasing with the number of subscribers in the network. As a result, 3G network was deployed. 3G first emerged in Japan in 2001, and the international telecommunications union (ITU) dictated several requirements for the 3G mobile system: CDMA 2000, wideband CDMA and time division synchronous code division multiple access (TD-SCDMA).

From today's commercial perspective, the CDMA 2000 1X system transports data transfer rates of 2.4 Mbps for indoor setting, and a maximum data throughput speed of 154 Kbps for outdoor and mobile environment. Systems including smart antennas, receive diversity and selectable method vocoder are the essential techniques to offer high throughput speed of 3G system. The cellular networks was expected to have a good internet utilization just like wired systems. Business companies started to urge the development of the 3G communities even before the primary industrial 3G network was integrated. The 4G cellular sites are expected to deliver improved solutions with a large throughput [1]. The innovative creation of mobile phone networks experienced huge achievements and was speedily implemented around the world. In the1990s,

CDMA air-interface system brcame an alternative to the 2G system. This was initiated by Qualcomm Inc, and the CDMA claimed 18 times more capacity than 2G GSM networks [2]. The mobile phone network model permits frequency reuse, so that each surrounding cell is permitted to utilize the similar bandwidth. Hence, CDMA offers the most effective use of the radio frequency resources. Frequency planning and designing, consequently, became obsolete for the CDMA cellular systems. Voice services received the most attention in the second-generation of wireless cellular systems, and the propagation of the Internet in the middle of the 90's caused the market to envision a system which could provide high transmission of data packets.

Multiuser detection deals with the simultaneous detection of multiple information streams, which are overlapping in both time and frequency. It uses all the active users' information to detect a single user data. Multiuser detection is mainly used in CDMA detection systems, which are widely in use nowadays in worldwide 3G cellular systems. It is similar to orthogonal multiple-access schemes such as the frequency division multiple-access (FDMA) and time division multiple-access (TDMA) systems.

In a CDMA channel, the communication quality is adversely affected not only by the additive thermal noise, but also by the multiple-access interference (MAI), which is caused by the other users simultaneously accessing the channel. Until the early 1980s, the straight approach to deal with multiple-access channels was to treat MAI as an additional Gaussian noise source, so that the conventional matched filter would be the optimal receiver. This approach, however, was shown to be wrong by Sergio Verdu, one of the pioneers of multiuser detection. Verdu derived the optimum minimum error

probability multiuser receiver in [3, 4], and showed that the near/far problem could be solved by resorting to detection algorithms taking into account the composition of the MAI. Multiuser detection has since generated a large volume of research from both industry and academia.

1.2. Multiuser Detection

CDMA system are known to rely on the spread spectrum techniques. In such systems, each data bit is multiplied by a wide band signal (code). This process is known as spreading, and the reverse operation is referred to as despreading. Despreading is the process that recovers the data bit by multiplying the received waveform by the designated code sequence. These codes are referred to as pseudo noise (PN) sequences, and usually designed to have certain features. The main property of these codes is the autocorrelation property, it minimizes the interference. Interference in CDMA can be intra-cell interference, or inter-cell interference. The former interference type occurs when the subscribers are served by the same cell, and the later one occurs by the nearby cells. The amount of interference in a CDMA system depends on the cross-correlation of the PN sequences for all active subscribers, and the spreading factor. Development of the CDMA technique, consequently, depends mainly on the spreading code properties. When orthogonal PN codes are employed, the interference would be minimum, when time synchronization exist.

The conventional detection (match filter) is the optimum detection in white Gaussian noise environment. However, this detection suffers from the near-far problem especially when MAI is present. If the interfering subscribers' signals are larger than that of the desired user, the match filter performance gets worse, and complex power-control

techniques are necessary to address the near-far issue, which is difficult in a real-time applications.

Multiuser detection (MUD) attempts to overcome the traditional near/far CDMA disadvantage at the receiver by cancelling most of the multiple access interference. Verdu [4] proposed such a system, which is known as the optimum maximum likelihood (ML) MUD system. Most of the planned MUD receivers could be categorized into two main groups: linear MUD and subtraction interference cancellation detectors. In the former, a linear transformation (modification) is applied to the output of the match filter to offer improved performance. In subtractive interference cancellation detectors, estimations of the interference will be created and iteratively taken out. Additionally, there are adverse group of methods which deal with the application of the multi-user techniques to practical scenarios.

1.3. Thesis Contributions

In this thesis we investigate MIMO systems and MIMO CDMA multi user detection receivers in Gaussian and non-Gaussian noise. We investigate the performance of the RSIC and RSTDD detectors in practical situations such as incomplete channel state information, correlated antennas, and impulsive noise. We propose a novel channel estimation robust detector. The results show that RSIC performs well under adverse conditions. We also show the results for V-BLAST detection criteria in impulsive noise channel modeled by Middleton's Class A type. We show the overall performance within various antenna designs and distinct noise factors. We then show the effect of the channel on the proposed systems. We propose a robust detection scheme (RDD), which improves the fading coefficient evaluation by enhancing the channel

matrix inside the system. Timing errors in the RDD are taken into account through the adjustment of the correlation matrix or the spreading code matrix. Consequently, the impulsive elements of the additive noise are processed via a robust nonlinearity to reduce the effect of the outliers. The results demonstrate that the performance of the RDD over the decorrelating detector is considerable. Additionally, we mention two main combining schemes and propose RSIC detector for the MIMO CDMA system. We also provide analytical results and carry out simulations to validate the analytical models, which consequently validate the gains realized by applying the proposed robust detection algorithm in a non-Gaussian noise environment [5, 6, 7, 8].

1.4. Thesis Outline

The contents of the thesis are organized as follows: Following the general introduction and our contributions in Chapter 1. Chapter 2 provides a literature review for CDMA detection algorithms.

Chapter 3 introduces the multiple-input multiple-output channel model. It also explains basic MIMO communication systems, such as VBLAST and MIMO CDMA. Chapter 4 provides the fading model overview. It also explains the impulsive noise models. Mathematical models for the impulsive noise, MIMO channel and fading effects are also stated in this chapter.

The analysis and design of our proposed robust detection is presented in Chapter 5. We state several robust detection algorithms for different settings. Timing mismatch, channel errors and impulsive noise are investigated. Chapter 6 validates the proposed results through simulations. Simulations are performed to either confirm the theoretical

derivations, or to show the performance gain in the proposed detection algorithms. Conclusions and key results of the thesis are summarized in Chapter 7.

Chapter 2

MULTIPLE ACCESS TECHNIQUES AND CDMA DETECTION ALGORITHMS

2.1. FDMA and TDMA

The simultaneous transmission in time and frequency is the fundamental idea behind the multiple access technique. One of these techniques is the FDMA. It allows frequency sharing by allocating a different carrier signal to every single subscriber so that the individual user's spectra do not overlap. Then by using bandpass filtering we enable different demodulation of each channel. In time division multiplexing TDMA, time is divided into slots allocated to each incoming signal in round-robin fashion. Demultiplexing is performed by merely switching on to the received signal at the appropriate times. The vital characteristic of frequency division and time division multi access techniques is that, the various users are working in separate non-interfering channels. These multi access techniques function by ensuring that the signals transmitted by a mixture of users are mutually orthogonal. Channel or other non-ideal effects may require the placing of guard times in TDMA and spectral guard bands in FDMA to prevent from co-channel interference.

2.2. CDMA

In contrast to either of the previous systems, CDMA enables parallel access over the entire frequency band for every single user. The data bits are spread with precise

patterns known as spreading codes (spread spectrum approach). The signals can be differentiated by allocating them individual spreading codes. One option is to use orthogonal codes to eliminate the interference completely. However, the transmitting channel usually destroys the orthogonality and multiuser interference (MUI) turns to deteriorate the system's performance.

2.3. Multiuser Detection in CDMA

The expansion of multiuser detection techniques was originally envisaged by Verdu for the simple Gaussian channel. Zvonar and Brady expanded the work to fading channels in the 1990s [9, 10], under some simplifying statement such as the perfect knowledge of the channel impulse response. Later work has expanded these to investigate issues of channel estimation problems. Direct-sequence CDMA (DS-CDMA) has the most widespread use among CDMA technologies, where data bits are multiplied by a unique codes. In a classical DS-CDMA system, the user's information bits are detected through a bank of correlators that correlate the complete received signal with the particular user's code (despreading) [11, 12].

One of the major drawbacks of the CDMA system is the MAI, which is a factor that limits the capacity and the performance of DS-CDMA techniques. MAI is caused by the correlation the spreading codes of users. This interference is the consequence of random time offsets among users' waveforms. Even though the MAI caused by any one user is usually negligible, alarge group of active users cause substantially degradation in the system. The effects of MAI are not taken into consideration when the conventional-classic detector is employed. The classical detector employs an indi-

vidual user detection approach in which every user is detected separately without the concern of other users. Due to the existing interference among users, an enhanced detection technique is required. This technique is known as multiuser detection or joint detection. In this technique, data from various users is used mutually to more effectively filter every specific user's data bit. This provides major advantages to the DS-CDMA systems.

2.3.1. Conventional Detection

A mathematical model for a synchronous DS-CDMA system is outlined. In synchronous CDMA, all bits for all users are synchronized in time. However, in realistic DS-CDMA systems, the wireless medium is generally asynchronous (for instance, waveforms are arbitrarily delayed). We assume that all carrier offset values are zero. When phases are also the same, the model allows us to utilize the baseband representation for real signals. To simplify further, we assume that no multipath effect is present, and the received signal arrives at the receiver through a single path. Assume a binary phase shift keying (BPSK) data modulation, with K DS-CDMA users in a synchronous BPSK real channel, the mathematical signal representation in baseband for the received signal can be stated as [13]:

$$r(t) = \sum_{k=1}^{K} A_k(t) S_k(t) b_k(t) + n(t), \tag{2.1}$$

where $A_k(t)$ is the amplitude of the user's signal, $S_k(t)$ is the spreading code, and $b_k(t)$ is the modulated signal of the k^{th} user, and $n(t)$ is additive white Gaussian noise (AWGN), that has double side power spectral density of $No/2$ W/Hz. The energy

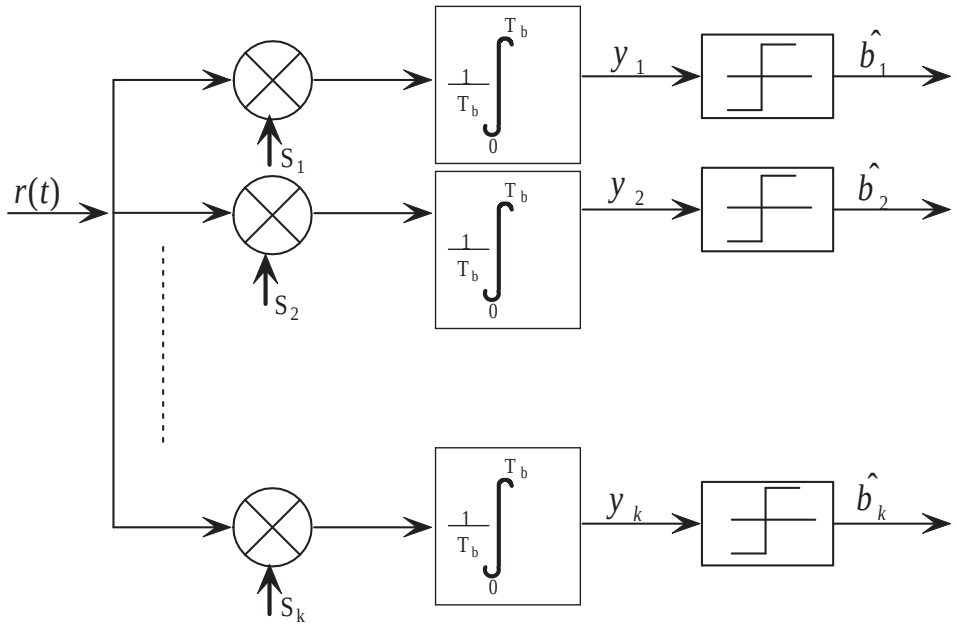

Figure 2.1. Block diagram of the match filter detection [13].

of the k^{th} signal is equivalent to the amplitude square, that is assumed not to change during the bit duration interval. The modulation is made up of rectangular signals of length T_b (bit period), which takes on $b_k = \pm 1$ values depending on the transmitted signal. The gold code or pseudo noise signal is composed of rectangular codes of timeframe T_c (chip time period), that pseudo randomly carry $S_k = \pm 1$ values [14, 15].

The conventional detector is shown in Figure 2.1, which is a group of K correlation devices. Every spreading sequence is generated and correlated with the received signal in a specific branch. The correlating detection process is known as matched filtering. The results of the match filtering process are sampled over the bit periods, providing "soft" estimates of the received signal. The remaining ± 1 "hard" information decisions are produced with respect to the sign of the soft data. It is obvious that classical detection pursues an individual data detection technique; every part discovers a single

individual with no consideration towards other users. Consequently, there is no joint detection of multiuser information or cooperative processing. The performance of this algorithm relies upon the features of the spreading sequence correlations. It is necessary that the correlations involving the identical code sequence (autocorrelations) are greater than the correlations among the other spreading-codes (cross-correlations). Mathematically, the correlation formula is described as [13]:

$$\rho_{i,k} = \frac{1}{T_b} \int_0^{T_b} S_i(t) S_k(t) dt, \tag{2.2}$$

where, if $i = k$, then $\rho_{k,k} = 1$. For $i \neq k, 0 < \rho_{i,k} < 1$. The outcome of the k^{th} user's correlator for a specific bit period is [13]:

$$y_k = \frac{1}{T_b} \int_0^{T_b} r(t) S_k(t) dt, \tag{2.3}$$

$$y_k = A_k b_k + \sum_{i=1(i\neq k)}^{K} \rho_{i,k} A_i b_i + \frac{1}{T_b} \int_0^{T_b} n(t) S_k(t) dt, \tag{2.4}$$

$$y_k = A_k b_k + MAI_k + z_k. \tag{2.5}$$

Note that codes are designed to reduce MAI (i.e., $\rho_{i,k} << 1$)

MAI has a considerable influence on the performance of the classical DS-CDMA system. The relation between MAI and the number of users in the system is directly proportional; the higher the number of operating users, the higher the MAI. Addition-

ally, higher power users worsen the detection of the lower amplitude users, as seen by (2.5). Therefore, the general influence of MAI on system efficiency is even more noticeable when users' signals are received at various energy levels. Lower amplitude users are dominated by high amplitude users, where such a circumstance occurs when the transmitters are in different topographical areas from the receiver. This is referred to as the near/far problem and fading could also contribute to these adverse effects outlined below:

1. *Interference flooring*: If the interferer signal is not absolutely orthogonal with the desired one, the result of the standard matched filtering will have multiple access interference. Therefore, even if we assume a zero AWGN on the system, bit error may still occur do to the MAI. This creates a problem in achieving low bit error rates.

2. *Near-far problem*: The IS-95 mobile network system utilizes strict power control methods to prevent this issue. However, these mechanisms have high cost and complexity.

2.3.2. Multiuser Detection

In joint detection systems or MUD, PN sequence and time details (and perhaps signal power or phase) of many users are mutually used to enhance the detection of every single user. The code sequences for a number of users are identified at the receiving side a priori. Some of the main multiuser detectors are described below:

2.3.2.1. Decorrelating Detector and MMSE Detector. This detection technique maps the output of the correlators using the inverse of the cross correlation matrix $\mathbf{R}^{-1}$, here

$\mathbf{R} = \rho_{i,k}$ is the $K \times K$ matrix (assuming synchronous CDMA) as described in (2.2). The output of bank of K matched filter outputs can be written as:

$$\mathbf{y} = \mathbf{RAb} + \mathbf{n}, \tag{2.6}$$

The decorrelating detector that results from the above mentioned process can be expressed as [13]:

$$\hat{\mathbf{b}} = sgn\left(\mathbf{R}^{-1}(\mathbf{RAb} + \mathbf{n})\right), \tag{2.7}$$

$$\hat{\mathbf{b}} = sgn\left(\mathbf{Ab} + \mathbf{R}^{-1}\mathbf{n}\right), \tag{2.8}$$

In order to perform the MMSE detection, $\mathbf{R}^{-1}$ is replaced in (2.7) by:

$$\mathbf{W} = (\mathbf{R} + \sigma_n^2\mathbf{A}^{-2})^{-1}, \tag{2.9}$$

where $\sigma_n^2\mathbf{A}^{-2} = diag\{\frac{\sigma^2}{A_1^2}, \frac{\sigma^2}{A_2^2}...\frac{\sigma^2}{A_k^2}\}$. Hence we observe that without any background noise the DD reaches ideal filtering and the detection level outperforms the classical filter. One benefit of the decorrelating detector is that it does not necessitate the prior knowledge of the obtained signal amplitude. It is clear that MAI will be entirely canceled (given that the inverse of the cross correlation matrix exists). The disadvantage is the consequence of noise amplification due to the multiplication of the cross correlation values $\mathbf{R}^{-1}$, with the noise as in $\mathbf{R}^{-1}\sigma_n^2$. This is typically more substantial

than that of the elements in σ_n^2. For this reason, the DD performs well as long as MAI dominates noise.

Minimum mean square error (MMSE) multiuser detection techniques is a trade off between the match classical filter and the decorrelator detector. It takes into account the interference and noise simultaneously.

When the noise is insignificant as compared to users interference, the matrix in (2.9) reduces into the cross correlating inverse matrix $\mathbf{R}^{-1}$. When the interference is insignificant, matrix $\mathbf{R}$ is diagonal and breaks to a group of scaling components on the correlator outputs that will not affect decisions on data at all. Actually, when there is no MAI, the results of the correlators would be the the best possible decision variables and does not require signal processing.

2.3.2.2. Subtractive Interference Cancellation Detectors. Subtractive interference cancellation detectors are categorized as an additional significant class of detectors. The essential property of these detectors is the formation of interference estimations, which is caused by every user, in order to eliminate some or all of the interference viewed by the other users. Frequently, these detectors are realized by multiple stages, and performance increases further with the stages. Hard or soft bit estimations can be applied to calculate the MAI. The soft choice is to use soft data estimates for the combined estimation of the data bits and amplitudes, and is simpler to employ. The nonlinear technique that includes feeding back bit decisions is known as the hard-decision method; it necessitates consistent estimations of the established user amplitudes so that we can produce estimates of users interference. Subtractive interference cancellation could

further be categorized as follows:

1. *Successive Interference Cancellation (SIC)*:

   SIC improves the bit error rate performance by generating estimations of the interfering data signal, and then cancelling regenerated interference from the original signal. This interference cancellation scheme outperforms the DD and the MMSE detectors when near far problem is dominant.

2. *Parallel Interference Cancellation (PIC)*:

   The PIC detector is similar to the SIC in generating estimations of the interfering signal, subtracting those regenerated interference from the original signal in parallel. Hence, the interference cancellation is immediate for all the users in the scheme. The multistage PIC construction was presented in [16]. The PIC depends mainly on the accuracy of MAI estimations, which depend on the data, channel coefficients, and offset estimates of the users. Any problems with these estimates would damage the efficiency of the PIC. Particularly imprecise complex channel coefficient estimations result in a large error on the MAI estimates.

3. *Zero-Forcing Decision-Feedback Detector (ZF-DF)*:

   In the ZF-DF system, also known as the decorrelating DF detection [17, 18], two processes are performed: linear processing and then a form of successive interference cancellation process. The linear function moderately decorrelates the signal while not amplifying the noise, where the SIC operation decides and eliminates the interference from a single excess user at a time. The ordering is done in decreasing order of the user's power. The ZF-DF detector utilizes

the SIC system to create the partially decorrelated bits. The initial result of the first bit of the 1st user, without any MAI, is employed to generate and subtract out the MAI it has, therefore, making the soft output of the first data bit of the 2nd user MAI free as well. This procedure carries on, for every time the process is iterating, the MAI brought by one added bit (the earlier decoded one) is generated and canceled.

4. *Hybrid Successive-Parallel Interference Cancellation (HIC)*:

   The HIC merges the SIC with the low delay of the PIC. A HIC scheme of PIC and SIC is initiated in [19], where two hybrid configurations are compared with SIC and PIC schemes. It is known that the hybrid IC scheme has more gain overall than PIC or SIC schemes. However, additional research is required for the optimum design, since it is shown that differences exist in the complexity and delay between the two hybrid configurations. In addition, the system used to select the users for the PIC stage needs to be improved further to enhance the BER performance.

5. *Groupwise Successive Interference Cancellation (GSIC)*:

   In the majority of groupwise detectors, users are either grouped according to their received powers or by their data rate (in the multirate case). In [20], GSIC method for a DS-CDMA system is discussed. The analysis of the GSIC model under BPSK modulation and Rayleigh fading asynchronous channel is available. The GSIC system leads to a sizeable decrease of the hardware complexity. Numerical outcomes demonstrate that the method performance of the GSIC system

reaches the efficiency of the SIC one, once the group size is not too large.

Chapter 3

MIMO COMMUNICATION SYSTEMS

3.1. Introduction

In radio communications, multiple-input multiple-output (MIMO) is the use of multiple antennas at the transmitting and receiving ends to improve the communication performance. It is a form of enhanced antenna system. MIMO technologies are the promising techniques in cellular telecommunications, because they conduct high transmission rate and link range with no extra frequency resources or higher transmitting energy. MIMO systems spread the available entire transmitting power by the array antennas to realize a gain that enhances the spectral efficiency, or to accomplish a diversity factor that increases the connection reliability by decreasing the fading effect. For these reasons, MIMO is an important aspect of the most recent mobile network standards, for example IEEE 802.11n, 4G, WiMAX, 3GPP LTE and HSPA+.

MIMO systems afford a linear increase of capacity with the number of antenna elements, providing considerable performance increases over single-input single-output (SISO) systems. To benefit from the performance of MIMO systems, the MIMO channel must be suitably modeled. It is customary to model the MIMO channel as an independent quasi-static flat Rayleigh fading channel. There are various methods that are usually used to MIMO techniques, such as the space time block codes (STBC)

[21, 22], space time trellis codes (STTC) [23] and bell-labs layered space time architecture (BLAST) [24]. In this framework, there is a large number of radio propagation models, each developed and used for special applications. The right depends on operational parameters such as the surroundings, velocity, accuracy, cost and simplicity of use. In general, experience has revealed that for scenarios and factors that are not available on-site, sufficient accuracy can be attained by simulations and stochastic models. On the other hand, for scenarios which are more specific, tracing models that utilize physical databases provide reasonable accuracy, but at the cost of processing time.

With growing demands on faster wireless communication services, such as high speed data packets, and internet solutions, communication system capacity received a great attention from the researchers in last decade. Whilst huge materials are available on improving user data rates by means of coding systems, however, they accomplish that by a trade off with overall data rate. The MIMO communication techniques attempt to obtain capacities near to the Shannon capacity values by utilizing multiple transmit and receive antennas, in addition to complex space time signal processing methods.

3.2. Diversity

MIMO is the first technique that utilizes a number of antennas at the receiver or the transmitter side. It could be employed to combat channel fading, or to transmit data at a higher rate. MIMO aims to improve the communication link by the transmission and reception of several replicas of information through independent fading paths. Hence, MIMO decreases the probability of simultaneous signal fades. The reception of replicas of the same information at the receiver is referred to as diversity. The number of independent replicas of the same information at the receiver is called the “diversity

order" or the "diversity gain" of the system. In MIMO system, the transmitting and receiving antennas form $N_T \times N_R$ (N_T is number of transmitters and N_R is the number of receivers) independent radio paths and by doing so, we can provide a full diversity gain. Diversity systems are mainly interesting in the case richly scattering channels, but the targeted transmitted rate is close to that of SISO system. In other words, the additional antennas of the MIMO system are used to have the same transmission rate of a SISO system.

The diversity performance is linearly proportional with the number of transmitting branches provided that the number of receiving branches is higher than or equal to the number of transmitting antennas. One of the general MIMO systems is the bell layered space-time system (BLAST), the BLAST is a narrowband point-to-point communication design for accomplishing great spectral efficiency. The diagonally layered space-time building is referred to as diagonal BLAST (D-BLAST) and utilizes several antennas at the transmitting and receiving ends, and a coding design that orders the block codes diagonally in space and time. Diagonal BLAST was proposed by Foschini [24] to utilize MIMO at both ends of a wireless network. Initially, the BLAST detection scheme was based on iterative interference cancellation.

Assuming a highly scattering Rayleigh channel, the capacity of the coding scheme is linearly proportional with the number of antennas, and 90% of the Shannon capacity can be achieved. The D-BLAST has a complex structure, however, the complexities of D-BLAST implementation gave rise to research that led to VBLAST, which is a modified version of BLAST [25]. There are two interference cancellation schems in

the detection process of the BLAST, specifically, zero-forcing (ZF) [26] and minimum mean squared error (MMSE) [27]. Vertical BLAST (VBLAST), is proposed in [28]. In VBLAST, each data stream uses only one transmit antenna but in D-BLAST, the data streams are rotated and each data stream encounters all transmitting antennas. VBLAST is a less complicated version of BLAST, it is more feasible but theoretically has worse performance. D-BLAST achieves higher diversity, but demands more complicated encoder and decoder.

Diversity methods are conventionally used in the base stations (BS). In the downlink, the BS transmits from two or more antennas, while in the uplink the BS receives information via several receiving antennas. The diversity approach is significant for systems having a comparatively small number of transmitting antennas that function at low SNR values. A main drawback of a MIMO scheme is that the transmitted signals from distinct antennas must be uncorrelated, and hence, the antenna elements must be adequately separated. It has been shown in the literature that the spacing between antenna elements must be greater than half of the wavelength of the transmitted signals. In practice, the spacing go over by three and even ten times the signal's wavelength. Therefore, the diversity schemes are popular for mobile/portable devices that have size limitations.

3.3. MIMO Channel Model

Figure 3.1 shows a simple basic MIMO channel. In the MIMO channel a complex data elements $\mathbf{b} = (b_1, b_2, \ldots, b_{N_T})^T$ is transmitted and a complex vector $\mathbf{r} = (r_1, r_2, \ldots, r_{N_R})^T$

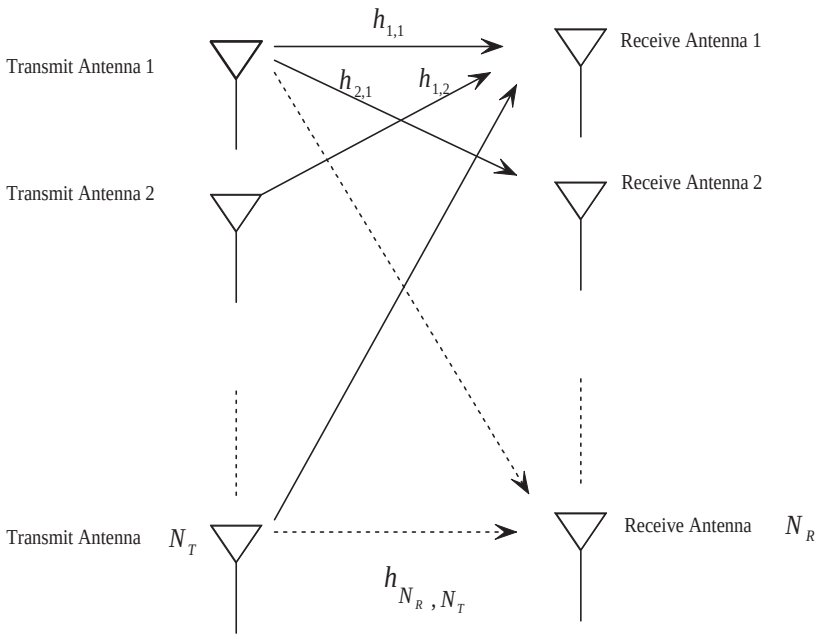

Figure 3.1. Block diagram of the MIMO channel.

is received. The input-output relationship can be expressed as in [21]:

$$\mathbf{r} = \mathbf{Hb} + \mathbf{n}, \tag{3.1}$$

where $\mathbf{H}$ is a $N_R \times N_T$ matrix addressing the multipath of the channel and $n = (n_1, n_2, \ldots, n_{N_R})^T$ is the noise. We assume that $\mathbf{H}$ is a randomly independent elements matrix with complex Gaussian distribution. We assume that the channel is constant over one symbol transmission and quasi-static fading channel, in other word, it may differ from one block to another. The channel coefficient $h_{i,j}$ is the path element from transmitting antenna j to receiving branch i. We presume that the channel elements are independently complex circular symmetric Gaussian random variables with zero mean and unit variance. It is also assumed that $\mathbf{H}$ and $\mathbf{n}$ are independent of one another and of the information vector $\mathbf{b}$. The block diagram of a VBLAST system is

shown in Figure 3.2, which has N_T transmitting branches and N_R receiving ones. The data stream is sub-divided into multiple streams and every substream is then modulated separately and directed through a different transmitting antenna.

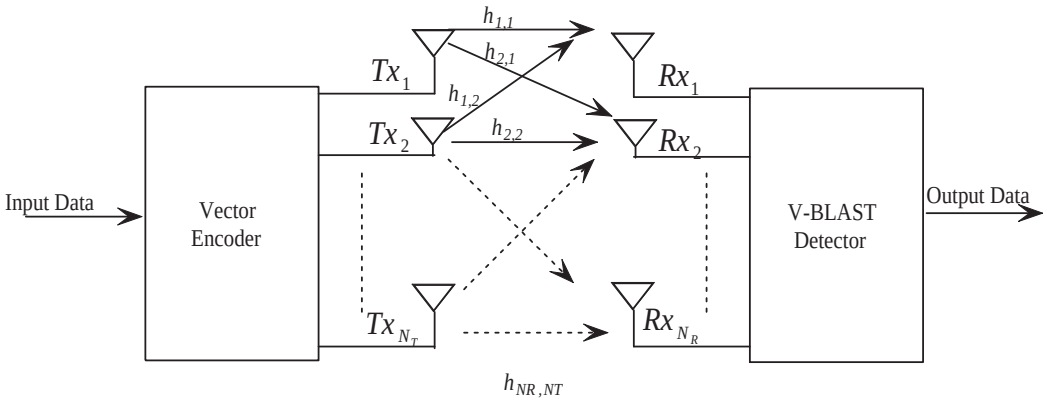

Figure 3.2. Block diagram of the VBLAST detector [25].

3.3.1. Alamouti's Scheme and Space-Time Coding

The transmit diversity technique proposed by Alamouti was the first space-time block codes (STBC) [21]. The encoding and decoding process is designed in sets of two modulated symbols. The STBCs are the simplest type of spatial sequential codes that develop the diversity with several transmitting antennas. Alamouti designed a straight forward transmission diversity method for systems having two transmitting antennas. This technique offers full diversity and necessitates simple linear process at both the transmission and the reception side. The encoding and decoding are performed with blocks of transmission symbols. Alamouti's simple transmit diversity system was extended in [29, 30] using orthogonal designs for larger numbers of transmitting antennas. These codes are known in the literature as orthogonal space-time block codes (OSTBCs).

Alamouti scheme can be described as follows: Let x_1, x_2 be the two modulated symbols that enter the space-time encoder. The times t_1, t_2 are separated by a constant time duration T. In the Alamouti structure, for the duration of the 1st time instance, the symbols x_1 and x_2 are transmitted by the 1st and the 2nd antenna correspondingly. While in the subsequent time instance t_2, the negative of the conjugate ($-x_2^*$) is sent by the 1st antenna while the conjugate of the 1st symbol (x_1^*), is transmitted from the second antenna.

3.3.2. Space-Time Trellis Codes

STBCs cannot attain the transmission rate of a SISO system when having several transmitting antennas. Furthermore, even though STBCs offer diversity, the capacity of the MIMO system is not completely exploited. It is possible to design codes that present not only diversity but also some coding gain, consequently, this will increase the complexity. More accurately, the code's complexity increases with the number of transmission bits and the modulation used, these codes are represented in the literature as space-time trellis codes (STTCs). These codes are based on the convolutional encoding practice presented in [23].

3.3.3. MIMO Detection Algorithms and VBLAST

The VBLAST encoding process is simple and is as follows: converting the data stream into streams (layers), then encoding the streams, finally, we transmit independently. DBLAST converts each code word into two blocks, A and B. At the first time slot, antenna 1 does not transmit and antenna 2 transmits A. During the remaining time slots, antenna 1 transmits B antenna 2 transmits A (if possible).

Assuming perfect channel estimation, the decoding at the receiver becomes achievable through the VBLAST algorithm. The detection and estimation of the transmitted symbols is achieved in a vector-by-vector basis. The algorithm works on each vector in a symbol-per-symbol basis by iteratively detecting and estimating the transmitted symbols. The algorithm is based on interference cancellation. For every receiving antenna, the signals from various transmitting antennas are superimposed. At the decoder, the layers are sorted in descending order of the received power and each layer is estimated by looking at the remaining layers as noise. The estimate is fed back to cancel its interference to other layers. This is similar to the successive interference cancellation process. Three consecutive phases take place:

- ZF or linear interference suppression through MMSE.
- Interference cancellation of the symbols detected.
- Reordering of the detection process through SNR post-detection.

The VBLAST steps are [26]:

$$\mathbf{W}_i = \mathbf{H}^{+}, \tag{3.2}$$

$$\text{for } i = 1, ...K, \tag{3.3}$$

$$k_i = \text{argmin}_{j \in k_1, ..., k_{i-1}} \left\| \mathbf{W}_{i,j} \right\|, \tag{3.4}$$

$$y_{k_i} = \mathbf{W}_{i,k_i}\mathbf{r}_i, \tag{3.5}$$

$$\hat{b}_{k_i} = Q\left(y_{k_i}\right), \tag{3.6}$$

$$\mathbf{r}_{i+1} = \mathbf{r}_i - \hat{b}_{k_i}(\mathbf{H})_{k_i}, \tag{3.7}$$

$$\mathbf{W}_{i+1} = \mathbf{H}^{+}_{\bar{k}_i}, \tag{3.8}$$

$$i = i + 1, \tag{3.9}$$

where $\mathbf{H}^{+}$ symbolizes the Moore-Penrose pseudo-inverse of the channel matrix $\mathbf{H}$, [25, 26], $W_{i,j}$ is the j^{th} row of W_i. $Q(.)$ is an estimator for the closest constellation level, and is a sign operation for BPSK signals. $\mathbf{H}_{k_i}$ indicates the k^{th} column of $\mathbf{H}$, $\mathbf{H}_{\bar{k}_i}$ refers to the matrix attained by nulling of the columns $k_1, k_2, \ldots, k_i$ of $\mathbf{H}$, and $\mathbf{H}^{+}_{\bar{k}_i}$ means the pseudo-inverse of $\mathbf{H}_{\bar{k}_i}$. (3.4) establishes the order of channels being recognized; (3.5) performs zeroing and determines the decision statistic; (3.6) pieces calculated decision statistic then produces the decision; (3.7) carries out canceling via decision feedback, and (3.8) figures the new pseudo-inverse to the up coming iteration.

3.4. MIMO CDMA System

The use of array antennas at the receiver is to achieve diversity reception only, where the multiple transmit antennas may be employed to realize diversity or transmitting at

high data rates. Antenna diversity is realistic, efficient and therefore is commonly utilized method to minimize the influence of fading. The conventional technique employs several antennas at the receiver and achieves combining using diverse schemes, or selections, this enhances the quality of the received signal. Based upon the complexity and the level of channel knowledge at the receiver, many diversity combining methods can be used. One such a diversity combining methods involves selection combining (SC), where the diversity depends on selecting a threshold. Combining to maximise the SNR is known as maximal ratio combining (MRC). Detecting the branches independently is known as post detection combining (PDC).

3.4.1. The Downlink MIMO CDMA Model

Consider a downlink MIMO CDMA where the spreading codes are known. As shown in Figure 3.3, the system has K users with N_R receive and N_T transmit antennas, which demodulate the KN_T independent data substreams transmitted from the base station. The mapper switches a specified user's data to a specific transmit antenna. The received baseband signal at the p^{th} receiving antenna which represents the p^{th} diversity reception is given by [31]:

$$r_p(t) = \sum_{m=1}^{M} \sum_{n=1}^{N_T} \sum_{k=1}^{K} c_{n,p} a_{k,n} s_k b_{k,n}(m) + n_p(t), \tag{3.10}$$

where $c_{n,p}$ is the fading coefficient of the n^{th} transmitting antenna and the p^{th} receiving one. $a_{k,n}$ is the amplitude of the k^{th} user from the n^{th} transmit antenna. $s_k \equiv s_k(t - mT_s - \tau_{n,p})$, is the spreading sequence of the k^{th} user. T_s is the symbol period. $\tau_{n,p}$ is the timing delay between the n^{th} transmitting and p^{th} receiving antenna. $b_{k,n}(m)$ is

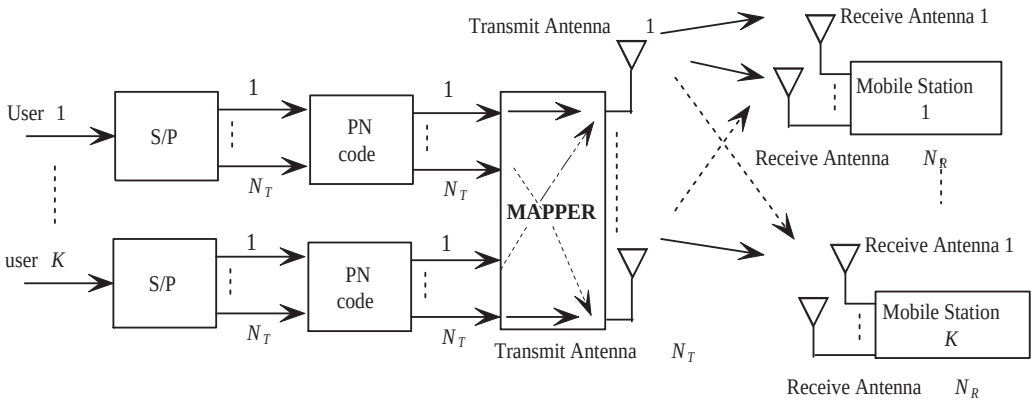

Figure 3.3. Block diagram of the downlink MIMO CDMA System [31].

BPSK modulated data. M is the frame size, and $n_p(t)$ is the noise term. The channel coefficients are zero-mean independent complex Gaussian random variables with unit variance. The discrete time matched filter signal at the p^{th} receiving antenna is:

$$\mathbf{r}_p = \mathbf{S}_p \tilde{\mathbf{C}}_p \mathbf{A}\mathbf{b} + \mathbf{n}_p, \tag{3.11}$$

where

$$\mathbf{S}_p = [\mathbf{S}_{k,n,p}(1)\ \mathbf{S}_{k,n,p}(2)\ \ \ldots\ \ \mathbf{S}_{k,n,p}(M)], \tag{3.12}$$

and

$$\mathbf{S}_{k,n,p(1)} = [\mathbf{s}_{1,1,p}(i) \ldots \mathbf{s}_{1,N_T,p}(i)\mathbf{s}_{2,1,p}(i) \ldots \mathbf{s}_{k,N_T,p}(i)], \tag{3.13}$$

$\mathbf{S}_p$ is the $MN \times KMN_T$ spreading code matrix formed by concatenating matrices in (3.13), $\mathbf{C}_p$ is $KMN_T \times KMN_T$ channel coefficients matrix formed by:

$$\mathbf{I}_M \otimes diag[c_{1,p}, c_{2,p}, \ldots, c_{N_T,p}],$$

where $\otimes$ denotes the Kronecker product. **A** is the $KMN_T \times KMN_T$ amplitude diagonal matrix. **b** is $KMN_T \times 1$ data vector:

$$\mathbf{b} = [\mathbf{b}_{k,n}^T(1)\ \mathbf{b}_{k,n}^T(2)\ \ldots\ \mathbf{b}_{k,n}^T(M)]^T, \tag{3.14}$$

where **n** is the $(M)N \times 1$ AWGN vector (or impulsive noise as it will be discussed later), and N is the spreading factor.

Chapter 4

FADING CHANNEL AND IMPULSIVE NOISE MODELS

Precise noise modeling is a key factor in signal detection, imprecise or inappropriate noise modeling presumptions turn out to be a problem in the system's performance [32, 33]. The additive noise channel model is the simplest communication model, which is illustrated in Figure 4.1. The transmitted signal $s(t)$ is degraded by an additive

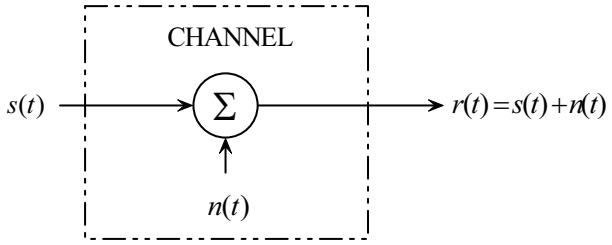

Figure 4.1. Additive Gaussian noise channel.

random noise process $n(t)$. This noise process may arise from interference during the movement in the propagation medium (in the case of wireless communications), or from the electronic mechanisms and the amplifiers at the receiver in the communication system (due to the electron's random motion). Because of this noise, the received signal $r(t)$ can be stated as:

$$r(t) = s(t) + n(t), \tag{4.1}$$

Thermal noise is the noise that is principally presented by the electronic devices, elements and amplifiers at the receiving end, and it may be statistically characterized as

additive Gaussian noise (AGN) process [34].

Even though AWGN channels are typically used as reference channel models in communication systems, they are inadequate for portraying communication channels in real-world scenarios, because there are diverse noise sources that may corrupt the transmitted signal, such as the impulsive noise.

4.1. Impulsive Noise Channel

4.1.1. Impulsive Noise Model parameterized by ϵ and κ

According to the central limit theorem (CLT), the noise results from the addition of many sources is typically modeled as Gaussian noise. However, this assumption is not valid all the time. There are some noise processes that exhibit non-Gaussian behavior, such as man-made noise, underwater acoustic noise, ... etc. [35, 36]. This type of noise can be modeled as impulsive noise, the probability density function (pdf) of an impulsive noise process is usually described using the Gaussian mixture model [37]:

$$f = (1-\epsilon)N(0,\sigma_n^2) + \epsilon N(0,\kappa\sigma_n^2), \tag{4.2}$$

Figure 4.2 shows the noise pdf tail that is substantial on the BER performance. As ϵ increases, the impulsiveness increases as depicted in Figure 4.3. The total noise variance is given by [38]:

$$\sigma^2 = (1-\epsilon)\sigma_n^2 + \epsilon\kappa\sigma_n^2, \tag{4.3}$$

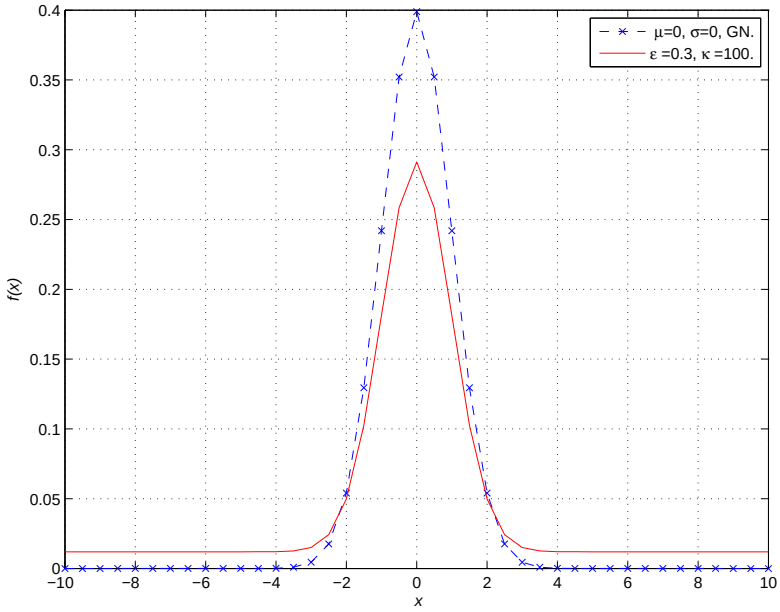

Figure 4.2. Impulsive noise pdf ($\epsilon = 0.2$, $\kappa = 100$), and GN pdf ($\mu = 0$, $\sigma^2 = 1$).

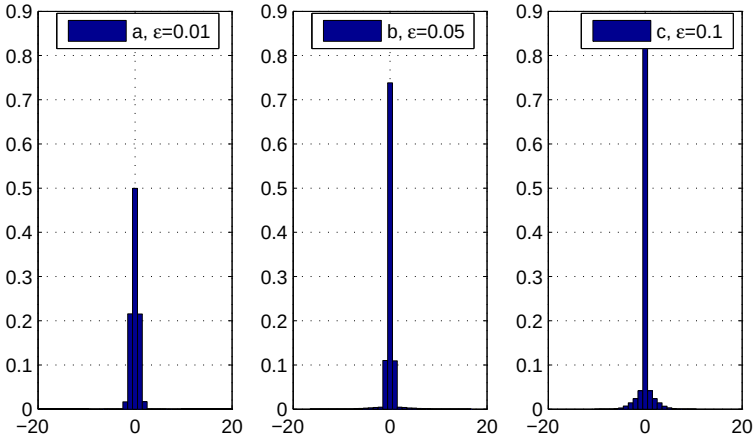

Figure 4.3. The impulsive noise histograms for various values of ϵ and $\kappa = 100$: (a) $\epsilon = 0.01$, (b) $\epsilon = 0.05$, (c) $\epsilon = 0.2$.

where $N(0, \sigma_n^2)$ is a Gaussian pdf with mean zero and variance σ_n^2, representing the effective background noise. $N(0, \kappa\sigma_n^2)$ shows the impulsive component, where ϵ is the probability to have an impulsive component and therefore $0 < \epsilon < 1$. κ is the strength

of the impulsive noise and $\kappa \geq 1$. The received signal with impulsive noise is given by (4.4), where $s(t)$ is the data signal and $n(t)$ is the impulsive noise content.

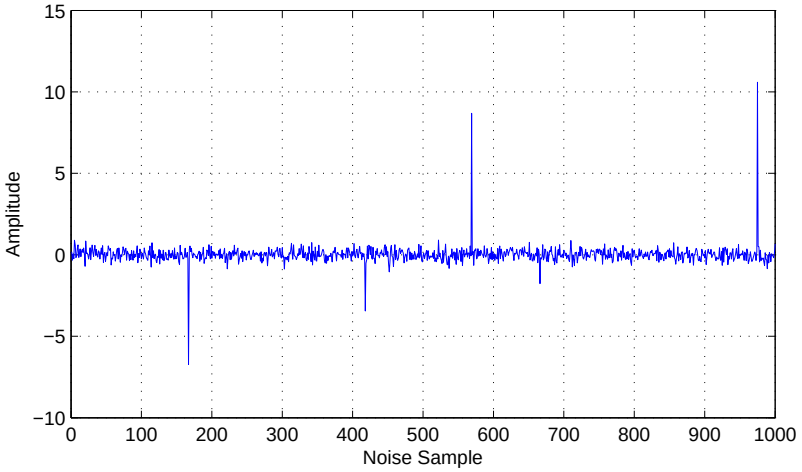

Figure 4.4. Impulsive noise sample, $\epsilon = 0.01$ and, $\kappa = 1000$.

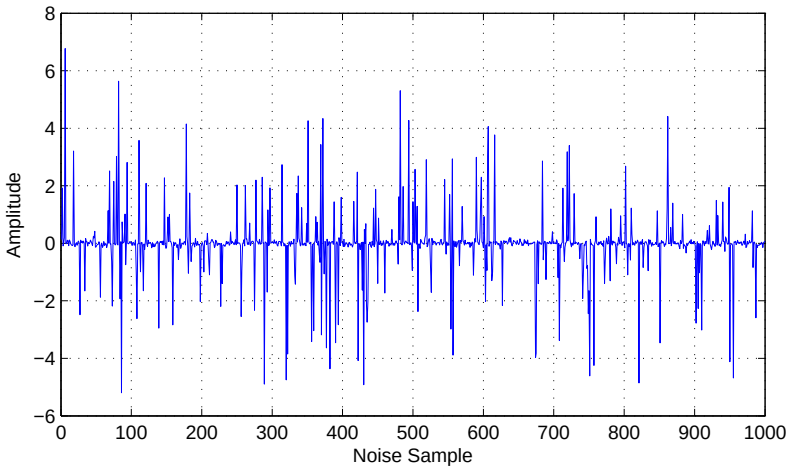

Figure 4.5. Impulsive noise sample, $\epsilon = 0.2$ and, $\kappa = 1000$.

$$x(t) = s(t) + n(t), \tag{4.4}$$

The tails of the impulsive noise distribution do not go to zero, but they do spread apart. Figure 4.4 and 4.5 show a sample of the noise model discussed above. As we

can clearly see, increasing the ϵ parameters will increase the number of impulsive parts in the sample.

4.1.2. Impulsive Noise Model Parameterized by X and Z

The second model assumption is Middleton's Class A type, which is parameterized by Z and X. This noise is made up of an infinite extension of Gaussian density functions with distinct variances and equivalent means [39]. This model assumes that each noise sample $n_s := g_s + i_s$ is the total of a background Gaussian part g_s, and impulsive portion i_s with $X := \mathrm{var}(g_s)/\mathrm{var}(i_s)$, standing for their power ratio. The pdf of the noise at any of the receiving antennas can be expressed as [40]:

$$p(n_p) = \sum_{m=0}^{\infty} \frac{\alpha_m}{\pi\sigma_m^2} exp(-\frac{|n_p|^2}{\sigma_m^2}), \tag{4.5}$$

where $\alpha_m = \frac{Z^m}{m!}exp(-Z)$. $\sigma_m^2 = \sigma^2(m/Z + X)/(X + 1)$, and $\sigma^2 = \mathrm{var}(n_p)$. Again X stands for the power amount of the background Gaussian noise and the impulsive component, and Z is the so-identified impulsive index. Small values of Z result in an impulsive behavior and a near-Gaussian when Z is significant [41, 42]. As certainly observed from its pdf in (4.5), the noise n_p is not Gaussian. Nevertheless, the class-A noise could be considered as conditionally Gaussian, also referred to as compound Gaussian, consequently, n_p , if conditioned on a poisson random variable Y_p with parameter Z, is Gaussian that has zero mean and variance presented as [40]:

$$v_p := \mathrm{var}(n_p/Y_p) = \sigma^2 \left(\frac{Y_p}{Z(X+1)} + \frac{X}{X+1} \right), \tag{4.6}$$

The variance of the noise n_p can be easily found by the expectation of (4.6) with respect to the random variable Y_p, using the fact that $E(Y_p = Z)$, where $E(.)$ denotes the expectation. The random variable Y_p controls the impulsive sample, if $Y_p > 0$ the impulsive component exists, and when $Y_p = 0$ there is no impulse component. Finally, we shall identify the joint distribution for the conditional variances $v_1, ..., v_{N_R}$, that lead to the distribution of n_p. In this case, two approaches can be used, one approach assumes that $(v_p, p = 1, 2, ..., N_R)$ are i.i.d random variables, whereas the second method assumes that $(v_1 = v_2 = ... = v_{N_R})$, and v_p is associated with a single poisson random variable. This assumption is valid when there is one physical process generating the impulsive noise, and this process affects different receiving antennas, thereby making the conditional variance v_p of the receive antennas equivalent to one another. This could possibly be a good model to a multi-antenna technique when the antenna branches are spaced closely. Statistically, $n_1, ..., n_{N_R}$ are dependent but uncorrelated [43]. This structure is often known as spherically invariant noise type and was applied in [44]. The noise samples joint distribution of the $\mathbf{n} := [n_1, ..., n_{N_R}]$ is [40]:

$$p(\mathbf{n}) = \sum_{m=0}^{\infty} \frac{\alpha_m}{(\pi\sigma_m^2)^{N_R}} e^{(-\sum_{p=1}^{N_R} \frac{|n_p|^2}{\sigma_m^2})}, \tag{4.7}$$

4.2. Fading Channels

The transmitted electromagnetic waves in mobile communications are deteriorated due to obstacles; such as mountains, trees, buildings and moving objects that hinder the line-of-sight (LOS) path. In addition to the LOS path, these obstacles result in reflected, diffracted, scattered and LOS signals that are vectorially summed to give one signal at the receiver. This result is called the multipath effect. Because of this mul-

tipath, the received signal is composed of the sum of delayed, attenuated, and phase-shifted multi-replicas of the transmitted signal. This accumulation could be constructive or destructive depending on the phase shift of each replica [45].

4.2.0.1. Flat Fading Channel. When the cellular radio channel bandwidth is higher than the bandwidth of the transmitted signal, the channel is known to be flat or frequency nonselective. The amplitude of the received signal varies with time, because of the variations in the channel gain. The distribution of the amplitude of a flat fading channel is important. The most common amplitude distribution is the rayleigh distribution [45]. The pdf of the rayleigh distribution is given as follow

$$p(x) = \begin{cases} \frac{x}{\sigma^2} e^{(-\frac{x^2}{2\sigma^2})} & , \quad 0 \leq x \leq \infty \\ 0 & , \quad \text{otherwise} \end{cases} \tag{4.8}$$

When the cellular radio channel bandwidth is smaller than the bandwidth of the carried signal, then the channel is frequency-selective. In this scenario, the impulse response of the channel carries a delay spread higher than the symbol interval on the transmitted signal. inter-symbol interference (ISI) in a frequency selective fading channel takes place because of the time dispersion of the transmitted symbols within the channel.

Chapter 5

ROBUST DETECTORS DESIGN

5.1. Robust Detection with Timing Mismatch and Channel Estimation Errors

In this section, we show the structure of the robust DD detector for timing mismatch and channel estimation errors. The RDD is used to detect the signals received by multi receiving antennas experiencing time mismatches. We research the performance of the detectors in practical situations such as incomplete channel state information, correlated antennas, and impulsive noise. We propose a novel robust detection. The results show that RSIC performs sufficiently well under adverse conditions [5].

Changes in the channel matrix will cause errors in the detection process. Timing errors in the system occurs when sampling at non-optimum sampling points. We consider timing mismatch of less than one chip duration. The spreading code vector $\mathbf{s}_{k,n,p}(i)$ can be expressed as two virtual spreading codes as in [46]:

$$\mathbf{s}_{k,n,p}(i) = \hat{\mathbf{s}}_{k,n,p}(i) + (\delta_{n,p} - \hat{\delta}_{n,p})\Delta\mathbf{s}_{k,n,p}(i) \tag{5.1}$$

where $\hat{\mathbf{s}}_{k,n,p}(i)$ is the estimated spreading code, $\Delta\mathbf{s}_{k,n,p}$ is the error in the estimated spreading code, $\delta_{n,p}$ and $\hat{\delta}_{n,p}$ is the true fractional part of the delay and the estimated one, respectively. Using adaptive algorithms, we try to minimize the error in the

spreading code matrix. Consequently, we improve the performance against timing mismatch. Similarly, the channel matrix $\mathbf{C}_p$ is also written in terms of two parts. Then, we minimize the error in the channel matrix, the system then will have few changes in some parameters. Such as extending the DD spreading code matrix $\mathbf{S}_p$ (by doubling the column size) to compensate the timing errors. Expanding the channel matrix $\mathbf{C}_p$ (by doubling the column and row size) to compensate the channel estimation errors, adjusting the amplitude matrix $\mathbf{A}$ and the data vector $\mathbf{b}$. This detector will use the estimated errors in the channel while deciding on the output data, and hence, it will have more information when deciding on each bit, so, it will improve the system performance. The received signal after these modifications can be written as:

$$\mathbf{r}_p = \mathbf{S}'_p \tilde{\mathbf{C}}'_p \mathbf{A}' \mathbf{b}' + \mathbf{n}_p, \tag{5.2}$$

where these modifications are given by:

$$\mathbf{S}'_p = [\mathbf{S}_{k,n,p}(1) \ \ldots \ \mathbf{S}_{k,n,p}(M)$$

$$\ldots \ \Delta\mathbf{S}_{k,n,p}(1) \ \ldots \Delta\mathbf{S}_{k,n,p}(M)],$$

$$\tilde{\mathbf{C}}'_p = [\hat{\mathbf{C}}_p \ \Delta\hat{\mathbf{C}}_p; \hat{\mathbf{C}}_p \ \Delta\hat{\mathbf{C}}_p],$$

$$\mathbf{A}' = I_{2\times M} \otimes \mathbf{a}',$$

$$\mathbf{b}' = [\mathbf{b}^T \ \mathbf{b}^T]^T,$$

$$\mathbf{a}' = diag(a_{1,1} \ \ldots \ a_{1,N_T} \ \ldots \ a_{K,N_T})$$

$$\tilde{\mathbf{C}}'_p = \hat{\mathbf{C}}_p + \Delta\tilde{\mathbf{C}}'_p, \tag{5.3}$$

where $\hat{\mathbf{C}}_p$ is the estimated channel matrix. When $\Delta\tilde{\mathbf{C}}'_p$=**0**, then the estimated channel matrix will match the true one. Now we perform maximal ratio combining and detect the signal at the receiver side, by multiplying (5.2) by $\mathbf{R}'^{-1}$, where $\mathbf{R}'^{-1}$ is :

By using the signal energy in the estimated code vector for bit detection, we have:

$$\hat{\mathbf{b}} = \hat{\mathbf{b}}'(1 : K \times M \times N_T),$$

where $\hat{\mathbf{b}}'(1 : K \times M \times N_T)$ is a vector consisting of the first $K \times M \times N_T$ elements.

For the RSIC and RDD, we use a clipper device to enhance the performance of the decorrelating detector in the impulsive noise scenario [47]. More specifically, a robust correlator is utilized so that each chip information goes through nonlinearity function (clipper) before the L chips make a bit, then it is delivered to a decision device. The model is developed for unfavorable effects by removing the excessive amplitudes that arise impulsively.

5.2. Robust SIC Detectoion for CDMA Systems in non-Gaussian Channels with Diversity Reception

The main contribution of our research is described in this section. We investigate and derive the BER performance of the SIC system under impulsive noise and maximal

ratio combining (MRC). We employ Middleton's class A type for the noise modeling [40]. Furthermore, we use PDC SIC detector as the robust multiuser detection technique to combat the impulsive noise at specific noise parameters in MIMO CDMA communication systems. We also show the performance of the system under near/far effect. We derive formulas for both combining techniques and demonstrate simulations in the next chapter.

In the literature, low complexity multiuser detectors have been proposed [48]. Some of these include the decorrelating detector [49], MMSE detectors, parallel and successive interference cancellation detectors, [50]. Multiuser techniques have mainly reduced the difficulty when the noise model is additive Gaussian. Wrong noise modeling would be a substantial problem [32, 33, 51].

In our work, we consider a simple SIC detector, which is a low complexity detector that limits the ordering to the average power, and does not require ordering after each cancellation. The complexity of this detector is $O(KN)$ and it is comparable to the classical match filter. The signal used to detect the user k is represented by [52]:

$$r(t)^k = r(t) - \sum_{i=1}^{K-1} \hat{s}_i(t - \tau_i), \tag{5.4}$$

where $\hat{s_k}(t) = \sum_{m=-\infty}^{\infty} \rho_{k,m} P_T(t - mT_s) S_k(t)$. $S_k(t)$ is the spreading code. $P_T(t)$ is a unit pulse signal outlined on $[0, T_s)$. $\rho_{i,m}$ is the received signal projection on the PN code of user i following the cancellation of the $(i-1)^{th}$ signal during the m^{th} symbol

time period, and given by [48]:

$$\rho_{k,m} = A_k b_{k,m} + \sum_{i=1}^{k-1} \hat{I}_{k,i,m} + \sum_{i=k+1}^{K} I_{k,i,m} + N_{k,m}, \tag{5.5}$$

where $N_{k,m} = \frac{1}{T_s} \int_{(m-1)T_s+\tau_k}^{mT_s+\tau_k} n(t) S_k(t-\tau_k) dt$. $I_{k,i,m}$ is the cross-correlation between spreading code k and other users signal, and $\hat{I}_{k,i,m}$ is the residual cross-correlation between signals after cancellation. Upon further analysis, a non iterative expression for the signal to interference and noise ratio (SINR) is found to be [52]:

where ϱ is given as [54]:

$$\varrho = \begin{cases} 1 \ , & \text{synchronous} \\ 2/3 \ , & \text{asynchronous} \end{cases} \tag{5.6}$$

The probability of bit error will be denoted as P_b. The average P_b for the k^{th} user is then calculated as:

$$P_k = Q\left(\sqrt{\Gamma_k}\right), \tag{5.7}$$

where $Q(t) = \frac{1}{\sqrt{2\pi}} \int_t^\infty e^{-x^2/2} dx$, and the average P_b of the system is taken to be the average P_b of all the users. Next, we discuss the impulsive effect on the detection process. First, we assume that the variance $\mathrm{var}(n_p/Y_p) = \sigma^2$ is the same for all the receive branches, $p = 1, ..., N_R$. Then, to determine the average P_b we have to evaluate the $E_{(\sigma^2,c)}\left[P_b(\Gamma_k|\sigma^2, c)\right]$, where $P_b(\Gamma_k|\sigma^2, c)$ is the P_b of the system over the channel c with noise variance σ^2. If $P_b(\Gamma_k|\sigma^2) = E_{(c)}\left[P_b\left(\Gamma_k|\sigma^2, c\right)\right]$ is the bits in error probabil-

ity averaged with respect to the random variable that describe the channel c, for a fixed noise variance, then the typical P_b of the MRC SIC detector under impulsive model is given by:

$$\begin{aligned} E_{(\sigma^2,c)}\left[P_b(\Gamma_k|\sigma^2,c)\right] &= E_{(c)}\left[\sum_{m=0}^{\infty}\alpha_m P_b\left(\Gamma_k|\sigma^2=\sigma_m^2,c\right)\right] \\ &= E_{(c)}\left[\sum_{m=0}^{\infty}\alpha_m Q\left(\sqrt{\Gamma|\sigma^2=\sigma_m^2,c}\right)\right] \\ &= \sum_{m=0}^{\infty}\left(\frac{1}{2}\right)\left(1-\sqrt{\frac{1}{1/\gamma_{|\sigma_m^2}+1}}\right)\alpha_m, \end{aligned} \tag{5.8}$$

where the random channel c, is a rayleigh random variable with the following distribution:

$$f(x) = xe^{-x^2/2}, \tag{5.9}$$

and $\gamma = \frac{1}{2}E[SNIR]$. (5.8) describes the P_b performance of the SIC detector in a SISO system. In a multi-receive antenna system, the signal is received and combined from all the antennas. Note that the individual amplitude of every received signal is rayleigh distributed. These N_R coefficients are independent and by using the properties of the Q function, we average $Q(\Gamma)$ with respect to the random channel coefficients as in [13]:

$$E\Big[Q\left(\sqrt{\Gamma}\right)\Big] = \frac{1}{2} - \frac{1}{2\sqrt{1+\gamma^{-2}}}\left(1+\sum_{n=1}^{N_R-1}\frac{1.3.5...(2n-1)}{n!2^n(\gamma^2+1)^n}\right) = B(\sqrt{\Gamma}), \tag{5.10}$$

Using (5.8), then P_b of MRC SIC detector with N_R receive antenna under impulsive

noise is:

$$P_{\text{MRCSIC}} = \sum_{m=0}^{\infty} \alpha_m B\left(\sqrt{\Gamma|\sigma = \sigma_m}\right), \tag{5.11}$$

Now, we will discuss the performance of the post detection combining successive interference cancellation (PDC). PDC is more robust against impulsive noise when the variance at each receiving branch is not the same, but i.i.d. The PDC detector determines preliminary hard decisions found out by sign$(c_p^* r_p)$ on each receiving antenna. The PDC then uses majority combining to make a decision. In our system, we assume that each receiving antenna executes a SIC detection and then we perform a majority combining. If there are equivalent numbers of +1's and -1's (when N_R is even), then the majority combiner chooses +1 or -1 at random with the same probability. Majority combining error in a PDC SIC detector will occur when more than $N_R/2$ decisions are wrong or when exactly $N_R/2$ branches are incorrect. Then, recalling (5.8) where the performance of the MRC SIC detector is shown (for SISO system), the P_b for the PDC SIC detection is (for even and odd N_R):

$$P_{\text{PDCSIC}} = \begin{cases} \sum_{k=N_R/2+1}^{N_R} \binom{N_R}{k} P_e^k (1-P_e)^{N_R-k} + \frac{1}{2}\binom{N_R}{\frac{N_R}{2}} P_e^{N_R/2}(1-P_e)^{N_R/2}, \text{even} \\ \sum_{k=(N_R+1)/2}^{N_R} \binom{N_R}{k} P_e^k (1-P_e)^{N_R-k}, \text{odd} \end{cases} \tag{5.12}$$

In all previous discussions, we assume that the variance at each receiving antenna is the same. Now, we derive bounds (exact analysis has high complexity) on the system

performance when the system employs different variance at every branch, and these variances are i.i.d. First, we will justify the use of equal variance or i.i.d at the receiving branch. In many applications, the array elements are placed far enough apart so that the noise field measured by the array elements is uncorrelated. However, it is not highly probable for the noise measured by different array elements to be statistically independent. Therefore, this equal variance model can be used to represent uncorrelated RV's in practical settings. On the other hand, the antenna elements might be separated from each other, and the variance at each receiving branch could be i.i.d. Hence, bounds are necessary to describe the system performance.

For simplicity, we assume that $\gamma^2 = A^2/\left(\sigma^2 + \sigma_I^2\right)$. Then using (5.10), the P_b conditioning on the channel fading amplitude is bounded by:

$$E_{(c)}\left[P_{\mathrm{MRCSIC}}(A^2|c)\right] \geq \frac{1}{2} - \frac{1}{2\sqrt{1+(\sigma^2+\sigma_I^2)/A^2}}, \tag{5.13}$$

We shall include the impulsive effect of the channel but we also note that the averaging of (5.13) will be according to the maximum value of the received variances $\sigma_{max}^2 = max\left(\sigma_{m1}^2, \sigma_{m2}^2 ... \sigma_{mN_R}^2\right)$. The probability mass function (pmf) of the resultant random variable is:

$$P(\sigma_m^2 = \sigma_{max}^2) = \left(\sum_{k=0}^{m} e^{-Z}\frac{Z^k}{k!}\right)^{N_R} - \left(\sum_{k=0}^{m-1} e^{-Z}\frac{Z^k}{k!}\right)^{N_R}, \tag{5.14}$$

Averaging (5.13) with respect to the maximum received variance using (5.14), we ob-

tain the following:

$$
\begin{aligned}
E_{\sigma^2_{max}}\left[P_{\mathrm{MRCSIC}}(A^2|\sigma^2_{max})\right] &\leq E_{\sigma^2_{max}}\left[\frac{1}{2}-\frac{1}{2\sqrt{1+(\sigma^2+\sigma_I^2)/A^2}}\right] \\
&\leq E_{\sigma^2_{max}}\left[\frac{1}{2}-\frac{1}{2\sqrt{1+\left(\frac{\sigma_m^2=\sigma^2_{max}+\sigma_I^2}{A^2}\right)}}\right] \\
&\leq \sum_{m=0}^{\infty}\left[\frac{1}{2}-\frac{1}{2\sqrt{1+\frac{\sigma_m^2+\sigma_I^2}{A^2}}}\right]P(\sigma_m^2=\sigma^2_{max}), \quad (5.15)
\end{aligned}
$$

Equation (5.15) represents an upper bound for the MRC SIC with i.i.d variances. Following a similar approach we may derive another bound on the performance of the PDC SIC detector. We show the derivations for an odd number of receivers (a similar model can be followed for even N_R). Recalling (5.12),

$$
\begin{aligned}
P_{\mathrm{PDCSIC}} &= \sum_{k=(N_R+1)/2}^{N_R}\binom{N_R}{k}P_e^k(1-P_e)^{N_R-k} \\
&\leq \sum_{k=\frac{N_R+1}{2}}^{N_R}\binom{N_R}{k}\left(E_c\{Q(A^2/(\sigma_m^2+\sigma_I^2))|c\}\right)^k \\
&\leq \sum_{k=\frac{N_R+1}{2}}^{N_R}\binom{N_R}{k}\left(\frac{1}{2}-\frac{1}{2\sqrt{1+\frac{\sigma^2+\sigma_I^2}{A^2}}}\right)^k \\
&\leq \sum_{m=0}^{\infty}\sum_{k=\frac{N_R+1}{2}}^{N_R}\binom{N_R}{k}\left(\frac{1}{2}-\frac{1}{2\sqrt{1+\frac{\sigma_m^2+\sigma_I^2}{A^2}}}\right)^k P(\sigma^2_{max}=\sigma_m^2), \quad (5.16)
\end{aligned}
$$

5.2.1. The Effect of the Powers of Residual Users

Throughout our discussion we highlighted the effects of the impulsive noise model for low complexity SIC detectors, ordering the power of the users after each cancellation

increases the performance of the system. However, when using PDC SIC algorithm ordering must be calculated N_R times, and hence, this process will be done discretely at each antenna. If (5.9) represents the amplitude distribution of the different users, then the pdf of the ordered user A_k (where A_1 is the strongest and A_k is the weakest) is denoted by $f_{A_k}(x)$, and obtained as [50]:

$$f_{A_k}(x) = \frac{K!}{(K-k)!(k-1)!} F^{K-k}(x) \left[1 - F(x)\right]^{K-k} f(x), \tag{5.17}$$

where $F(x)$ denotes the cumulative distribution function of $f(x)$. The error probability after the j^{th} cancellation is given as:

$$P_e^{j+1} = \int_0^\infty Q(\Gamma_{j+1}) f_{A_{j+1}}(x) dx, \tag{5.18}$$

In order to include the effect of the impulsive channel, we average (5.18) with respect to the impulsive noise variance distribution and obtain:

$$P_e^{j+1} = \sum_{m=0}^{\infty} \alpha_m \left(\int_0^\infty Q(\Gamma_{j+1}) f_{A_{j+1}}(x) dx \right), \tag{5.19}$$

We obtain the average of the error probability of the system using the averaging of the P_b from all cancellation stages. The resulting P_e of the system can be easily substituted into (5.12) to get the theoretical P_b of the PDC SIC system.

5.2.2. System Complexity

In the DD schemes, the inversion of the cross correlation matrix (**R**) is required. This matrix has $MK \times MK$ dimension, as the number of users K increases, the matrix

inversion process becomes complex. In addition, the channel coefficients, noise parameters, and the spreading codes are required for all the users. The computational complexity for such detectors is $O(M^3K^3)$, where the symbol $O(.)$ stands as a function for the number of floating points operations.

SIC detector, is a low complexity suboptimum CDMA detector, that can be considered as a practical detector for CDMA systems. Assuming that a multistage SIC scheme is used, and the number of stages is (J), the complexity of such a detector is $O(JMNK)$ [53], which is much lower than that of the DD. However, the SIC is assumed to converge in reasonable number of stages.

In the MRC SIC detector, the signals coming to all the receiving antennas are combined and the SIC scheme is performed. Assuming a MIMO CDMA system of $N_T \times N_R$, the MRCSIC computational complexity is $O(JN_TMNK)$. In PDC SIC detection, the SIC algorithm is performed at each branch, and hence this increases the complexity by a factor of N_R. So the computational complexity for the PDCSIC detector is $O(JN_TMNK)$. Moreover, if we use more complex SIC detectors, which include ordering of the users at every cancellation stage, or ordering considering the cross correlation between the spreading codes of the users, the complexity would be substantial.

In our model, we used a diversity reception system, so that the MIMO CDMA configuration is $1 \times N_R$. Moreover, no multi stage consideration was assumed, and no power ordering after the cancellation was also used. Consequently, the computational complexity for the MRCSIC is $O(MNK)$, and independent of the number of the receiving branches. The computational complexity of the PDCSIC is $O(MNKN_R)$.

Consider the example of a 1×4 MIMO CDMA system, for 5 users, 4 bits frame, and 31 spreading length. The number of additions/subtractions for the MRCSIC detector is approximately MKN, and the number of multiplications is $2NMK$, giving a total of 620 additions and 1240 multiplications. For a PDCSIC the number of additions/subtractions is approximately $N_R MKN$, and the number of multiplications is $2NMKN_R$, giving a total of 2480 additions and 4960 multiplications. As shown, the computational complexity for the PDCSIC is substantial.

5.3. Analysis of the DD and RDD for CDMA Systems in Non-Gaussian Channels

This section investigates the performance of the decorrelating detector in MIMO-CDMA system under two different impulsive noise models. We examine Middleton's class A noise type for the impulsive noise, and we derive the expression for the BER. We propose a robust detection technique to overcome the impulsive effect on the system. Throughout this part, we use MRC and PDC to achieve diversity reception. For these combining techniques, we present design and analytical results. The simulation results will be shown in the next chapter.

Multiple transmit antennas may be employed to achieve diversity or transmitting at high data rates, where it provides only diversity at the reception side. Receive diversity is a greatly used technique for eliminating the fading effects. In many physical channels, just like indoor [55], urban [24] radio channels and underwater acoustic channels, the ambient noise is known to be non-Gaussian, due to the impulsive man-made electromagnetic disturbance and natural noise as well [24, 56].

In this section, we consider the performance offered by the decorrelating detector in

a channel corrupted by additive noise that contains occasional outliers. Depending on the high-amplitude outliers, the capacity of a linear DS-CDMA receiver may degrade significantly [51]. We investigate and derive the probability of error expressions for the decorrelating detector, assuming a non-Gaussian noise model and different receive diversity orders.

5.3.1. The System Model

We consider a downlink MIMO CDMA, where the PN codes are known at the receiving end. The 1st impulsive noise type is the frequently applied Gaussian mixture model which is parameterized by ϵ *and* κ and was extensively used in [51, 57]. We adopt the usually employed two-term Gaussian mixture type. The probability density function of this noise structure is expressed as [38]:

$$p(n) = (1-\epsilon)G(0,\nu^2) + \epsilon G(0,\kappa\nu^2), \tag{5.20}$$

with $\nu > 0$, $0 \leq \epsilon \leq 1$ and $\kappa \geq 1$, where the $G(0,\nu^2)$ expression symbolizes the nominal background noise and the $G(0,\kappa\nu^2)$ expression presents the impulsive elements. $G(0,\nu^2) = \frac{1}{\sqrt{2\pi\nu^2}}e^{-n^2/2\nu^2}$, ϵ represents the probability that impulses occur (drawn from uniform distribution). It is typical to analyze the consequences of variation on the noise distribution by choosing the parameters ϵ and κ and with fixed overall noise variance [38]:

$$\sigma^2 = (1-\epsilon)\nu^2 + \epsilon\kappa\nu^2, \tag{5.21}$$

This noise model serves as an approximation to the more fundamental Middleton class A noise model [57, 58], and has been used extensively to model physical noise arising in radio and acoustic channels.

The second model assumption is Middleton's class A type parameterized by Z and X, and made up of an infinite extension of Gaussian density functions with distinct variances and equivalent means [39]. The pdf of the complex component noise at any of the receiving antennas can be expressed as [40]:

$$p(n_p) = \sum_{m=0}^{\infty} \frac{\alpha_m}{\pi \sigma_m^2} e^{\left[-\frac{|n_p|^2}{\sigma_m^2}\right]},$$

$$\alpha_m = \frac{Z^m}{m!} e^{(-Z)},$$

$$\sigma_m^2 = \sigma^2(m/Z + X)/(X + 1), \tag{5.22}$$

where $\sigma_m^2 = \sigma^2(m/Z + X)/(X + 1)$, and $\sigma^2 = \mathrm{var}(n_p)$. As certainly observed from its pdf in (5.22), the noise n_p is not Gaussian. but conditionally Gaussian and variance presented as [40]:

$$v_p = \mathrm{var}(n_p|Y_p) = \sigma^2 \left(\frac{Y_p}{Z(X+1)} + \frac{X}{X+1} \right), \tag{5.23}$$

The noise samples joint distribution of the $\mathbf{n} := [n_1, ..., n_{N_R}]$ is [40]:

$$p(\mathbf{n}) = \sum_{m=0}^{\infty} \frac{\alpha_m}{(\pi\sigma_m^2)^{N_R}} e^{\left[-\sum_{p=1}^{N_R} \frac{|n_p|^2}{\sigma_m^2}\right]} \tag{5.24}$$

Note that the first ϵ and κ noise type has been applied to model actual noise occurring in radio and acoustic environments, and has a constant impulsive probability. However, the second one has a number of impulses that are poisson distributed, and this model is more efficient to model the MIMO antenna systems.

5.3.2. Robust MIMO CDMA Detector

The received signal is filtered by by a match filter to form the sufficient statistics of the data vector, where **R** and **n** is the correlation matrix and the effective noise vector respectively, expressed by [31]:

$$\mathbf{y} = \mathrm{Re}[\sum_{p=1}^{N_R} \tilde{\mathbf{C}}_p^H \mathbf{S}_p^T \mathbf{r}_p] = \mathbf{RAb} + \mathbf{n}, \tag{5.25}$$

where

$$\mathbf{R} = \sum_{p=1}^{N_R} \tilde{\mathbf{C}}_p^H \mathbf{S}_p^T \mathbf{S}_p \tilde{\mathbf{C}}_p,$$

$$\mathbf{n} = \sum_{p=1}^{N_R} \tilde{\mathbf{C}}_p^H \mathbf{S}_p^T \mathbf{n}_p, \tag{5.26}$$

Multiplying (5.25) by $\mathbf{R}^{-1}$ and taking the sign of the result achieves space time decorrelation, also known as STDD. For the impulsive noise effects (ϵ and κ), a clipper is

used to improve the performance of the decorrelating detector [59]. In particular, we use a robust correlator in which each chip passes through a robust nonlinearity before comprising a bit and forwarded to a decision device. The decision of the clipper function is:

$$x = \begin{cases} \beta \ , & x > \mu \\ x \ , & -\mu < x < \mu \\ -\beta, & x < -\mu \end{cases} \tag{5.27}$$

If the sample x passes a threshold value μ then x is clipped to β, and if the sample x is less than -μ, then x is clipped to -β, else if $(-\mu < x < \mu)$ x remains as it is.

5.3.2.1. Asymptotic Performance Of The Decorrelating Multiuser Detector. At the receiver side, we multiply the received signal by the specific user spreading code S_k for despreading, and $\mathbf{R}_{k,k}^{-1}$ to remove the MAI from the other users. The spreading sequence has the two equiprobable random values $1/\sqrt{N}, -1/\sqrt{N}$. Now, consider the Gaussian mixture noise model given by (5.20), so that the received signal has the N-fold convolution of the following pdf:

$$p(w) = \sqrt{N} \times \left[\frac{(1-\epsilon)e^{-(w)^2 N/2\sigma_1^2}}{\sqrt{2\pi\sigma_1^2}} + \frac{(\epsilon)e^{-(w)^2 N/2\sigma_2^2}}{\sqrt{2\pi\sigma_2^2}} \right], \tag{5.28}$$

Using (5.28) and denoting the N-fold convolution of $p(w)$ as $P_N(w)$ we can write the received signal distribution $f(t) = \frac{P_N(w/\mathbf{R}_{k,k}^{-1})}{|\mathbf{R}_{k,k}^{-1}|}$. Substituting the relevant values of N and the correlation term $\mathbf{R}_{k,k}^{-1}$, we can generate the theoretical BER curves for a specific user.

However, another approximation for the P_e function was shown in [38], the asymptotic bit error probability for the class of decorrelating detectors for significant processing gain $N \to \infty$. Using the asymptotic normality condition, the asymptotic probability is:

$$P_e = Q\left(\frac{A_k}{v\sqrt{\mathbf{R}_{k,k}^{-1}}}\right), \tag{5.29}$$

where $Q(t) = \frac{1}{\sqrt{2\pi}}\int_t^\infty e^{-x^2/2}dx$. Then for N_R receiving diversity with MRC combining, the asymptotic probability of error becomes:

$$P_e = Q\left(\frac{\sqrt{\sum_{i=1}^{N_R}|A_{ik}|^2}}{v\sqrt{\mathbf{R}_{k,k}^{-1}}}\right), \tag{5.30}$$

Now, we discuss the performance of the decorrelating detector by applying a robust non-linearity given by (5.27), so the received signal distribution due to clipping can be written as:

$$p(t)_{\text{clipped}} = \begin{cases} \alpha\delta(t-\mu) \ , & t > \mu \\ sc(t) \ , & -\mu < t < \mu \\ \alpha\delta(t+\mu), & t < -\mu \end{cases} \tag{5.31}$$

where $\alpha = (1 - \int_{-\mu}^{\mu} sc(t)dt)/2$, and $sc(t)$ is the received signal distribution before clipping. Again, when filtering the received signal, we have the N-fold convolution of

the following pdf:

$$p(t)_{\text{matched}} = \sqrt{N}\left(p(\sqrt{N}t)_{\text{clipped}} + p(-\sqrt{N}t)_{\text{clipped}}\right), \tag{5.32}$$

And when determining the k^{th} user BER, the $\mathbf{R}_{k,k}^{-1}$ term will be included in the result, so that the finalized pdf is:

$$p(t)_k = \frac{1}{|\mathbf{R}_{k,k}^{-1}|} P(t/\mathbf{R}_{k,k}^{-1}), \tag{5.33}$$

where $P(t)$ is the N-fold convolution of (5.32). Once again, the probability of error for the class of decorrelating detectors for large processing gain $N \to \infty$, can be given by (5.29).

Next, we discuss the performance of the system under the(X and Z) impulsive noise model given in (5.22), there are two cases for this noise model.

1. When $\text{var}(n_p|Y_p) = v$ is the same for all the receive antennas $p = 1, \ldots, N_R$.
2. When $\text{var}(n_p|Y_p) = v_p$ is different for all different receive antennas, but i.i.d, as described in (5.23).

For BER analysis we will adopt the first case, because the second case requires complex calculations. However, we will demonstrate the performance simulations for both cases in the next chapter. To determine the average BER, we have to evaluate the $E_{v,c}[\text{BER}(A|v,c)]$, where BER $(A|v,c)$ is the BER of the system over the chan-

nel c with noise variance v. The regular BER forms for fading channels over constant variance are known for most diversity combining systems [40]. If $\mathrm{BER}(A|v) = E_c[\mathrm{BER}(A|v,c)]$, is the bits in error probability averaged with respect to the random variable that describe the channel c for a fixed noise variance, then the typical P_b of the MRC detector under impulsive model is given by:

$$P_e = E_{v,c}[\mathrm{BER}(A|v,c)] = E_v[\mathrm{BER}(A|v)]$$

$$= \sum_{m=0}^{\infty} \alpha_m Q\left(\frac{A_k}{(v=\sigma_m)\sqrt{R_{k,k}^{-1}}}\right), \tag{5.34}$$

We will bound the probability of error. In (5.34), we represent the specific average BER for (X and Z) impulsive noise fading channels. However, it is possible to proceed with (5.34) in order to have a bound, so, we use the average BER of any diversity combining system with diversity order N_R for a fixed noise variance v is limited by [40]:

$$\mathrm{BER}(A|v,c) < G_c(A/v)^{-N_R}, \tag{5.35}$$

where G_c and N_R are known as the coding and diversity gain respectively. Note that (5.34) is applicable to the performance of any diversity combining approach with distinct values of Gc and N_R related to the various combining systems. Taking into ac-

count the expectation of both sides in (5.35) and undertaking further processing [40]:

$$\mathrm{BER}(A|v,c) < G_c(A/\sigma^2)^{-N_R} \times \sum_{i=0}^{N_R} \begin{pmatrix} N_R \\ i \end{pmatrix} \frac{E[Y^i]}{Z^i(X+1)^i} \left[\frac{X}{X+1}\right]^{N_R-i}, \quad (5.36)$$

Finally, one should note that v in (5.34) may not be the same for all the receiving antennas, but they are i.i.d random variables as in [43]. In this case, post detection combining is a robust technique and performs quite well under these circumstances. In (PDC) the PDC receiver first determines hard decisions presented by $\mathrm{sign}(\mathbf{R}^{-1}\mathbf{y})$ for every antenna followed by a second decision using majority combining.

Chapter 6

SIMULATIONS RESULTS

6.1. VBLAST System

In this section, we show the VBLAST performance in impulsive noise environment described by Middleton's class A type (parameterized by X and Z) with BPSK signalling in a highly scattered Rayleigh-fading MIMO channel. The performance is described by the mean of bits in error in the system (BER). We examine various antenna options and distinct noise variables. We apply Monte Carlo simulation technique to confirm the performance evaluation. This simulation displays the overall performance for different numbers of antenna configurations, and we assume perfect channel knowledge at the receiver. The following simulation settings are used:

- Middleton's class A type (parameterized by X and Z).
- BPSK modulation and Rayleigh-fading MIMO channel.
- Perfect channel knowledge at the receiver is assumed.
- The SNR is before the channel combining.
- The impulsive ratio is $X = 0.1$.

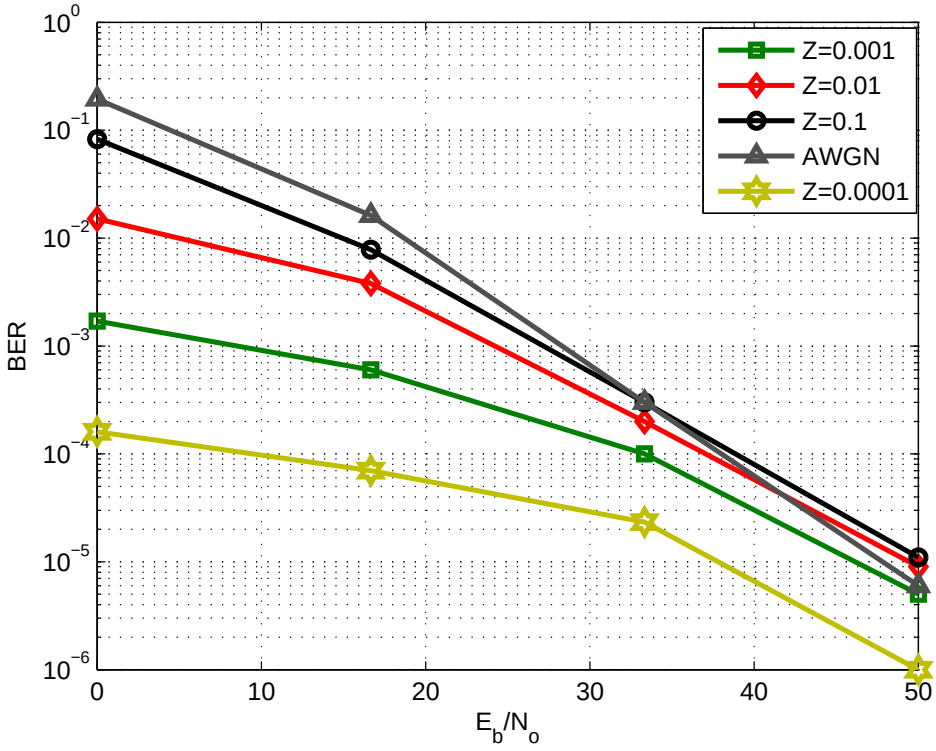

Figure 6.1. BER versus SNR for (2×2) MIMO system, impulsive noise with different values of Z and AWGN, equal variance at each receive antenna, $v_1 = v_2 = ... = v_N$.

Figure 6.1 depicts the performance of the 2×2 system, the simulation curves represent the BER at a given SNR. We used equal variance at each receiving antenna, $v_1 = v_2 = ... = v_N$. The BER curve for AWGN channel is also shown as a reference. The curve where $Z = 1$, is very close to the reference AWGN one, that is why it is called near Gaussian case. When Z approaches 1, the performance inches closer and closer to the AWGN reference. The less the value of Z is the higher the impulsive noise is.

Figure 6.2 shows the performance of the 2×2 system with i.i.d noise variance. As SNR increases, performance at AWGN case goes to less BER values faster than the case of highly impulsive noise. In Figure 6.3, 4×4 system is shown, the variance at each receive antenna is i.i.d, and this will cause higher deterioration in the BER.

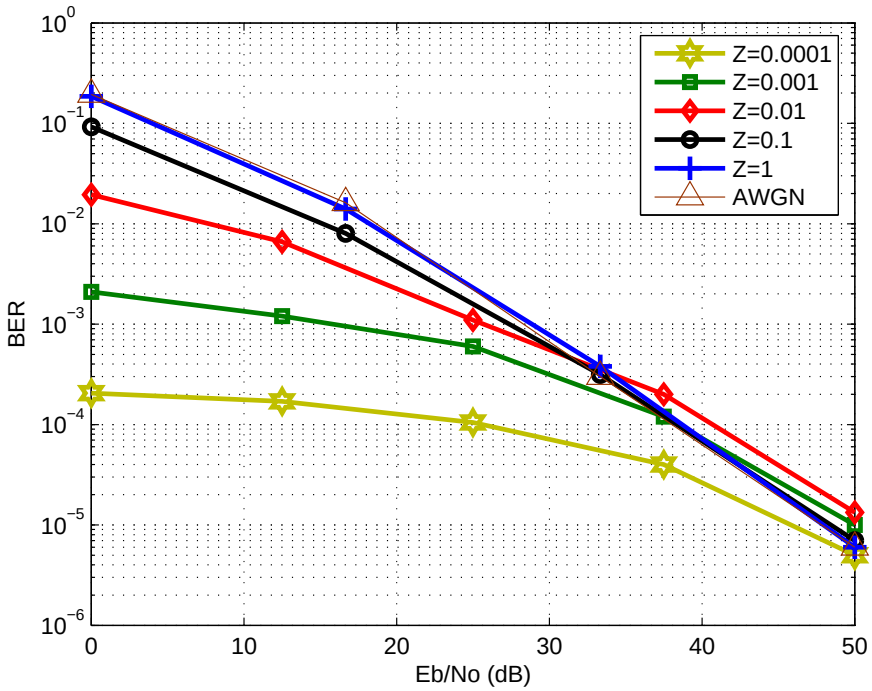

Figure 6.2. BER versus SNR for (2×2) MIMO system, different values of Z, AWGN, and variancees are i.i.d.

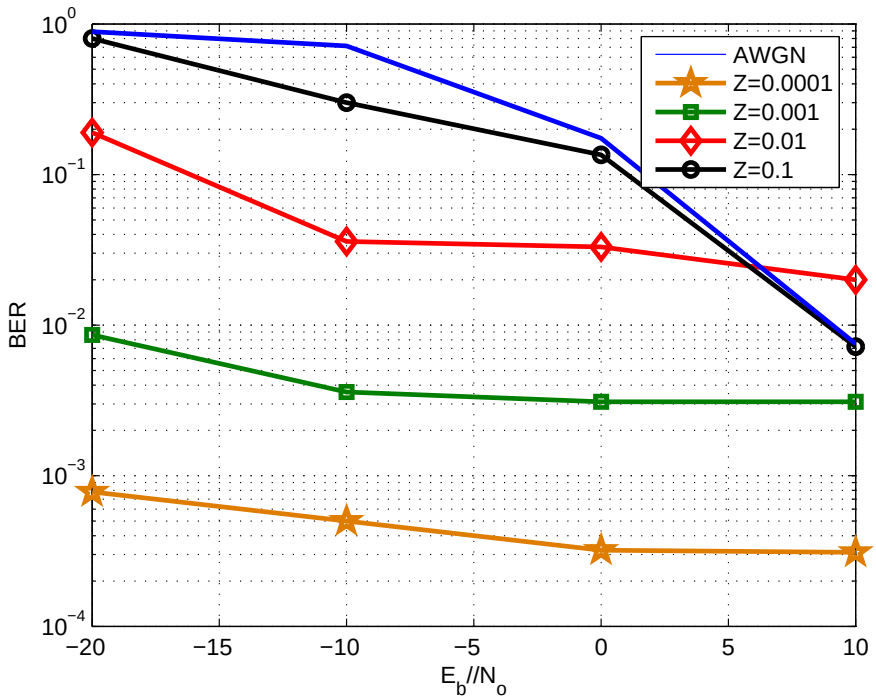

Figure 6.3. BER versus SNR for (4×4) MIMO system, different values of Z, AWGN, and variancees are i.i.d.

This is due to the fact that when the noise samples are independent at different receiving antennas, the total power of the noise after combining is higher than that in the dependent noise sample case. The highly impulsive noise case occurs when $Z = 10^{-4}$. In cases with high impulsive noise case, the background noise is decreased, which explains the low BER at low SNR. When the SNR is high the effect of the impulsive noise appears, and the BER is deteriorated, this agrees the results in [40].

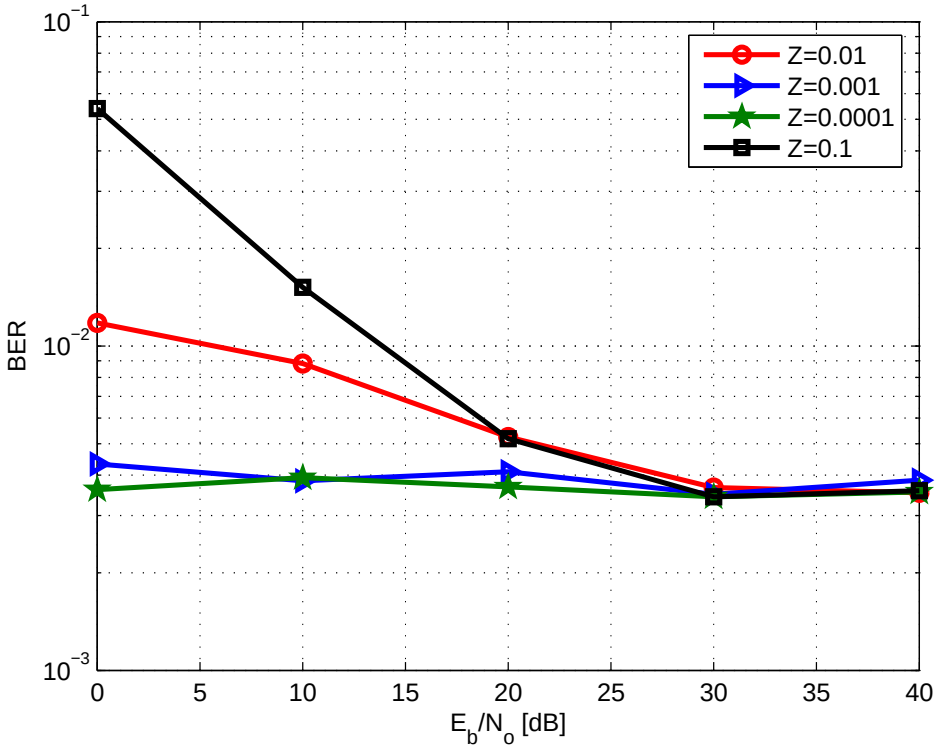

Figure 6.4. BER versus SNR for (2×2) MIMO system, impulsive noise with different values of Z and 10% channel estimation error, same variance at each receive antenna,

$$v_1 = v_2 = ... = v_N.$$

If the channel is not perfectly estimated at the receiver, the VBLAST detection is heavily deteriorated. This can be easily seen in Figure 6.4 and 6.5, where the error between the actual channel and the estimated one is 10%.

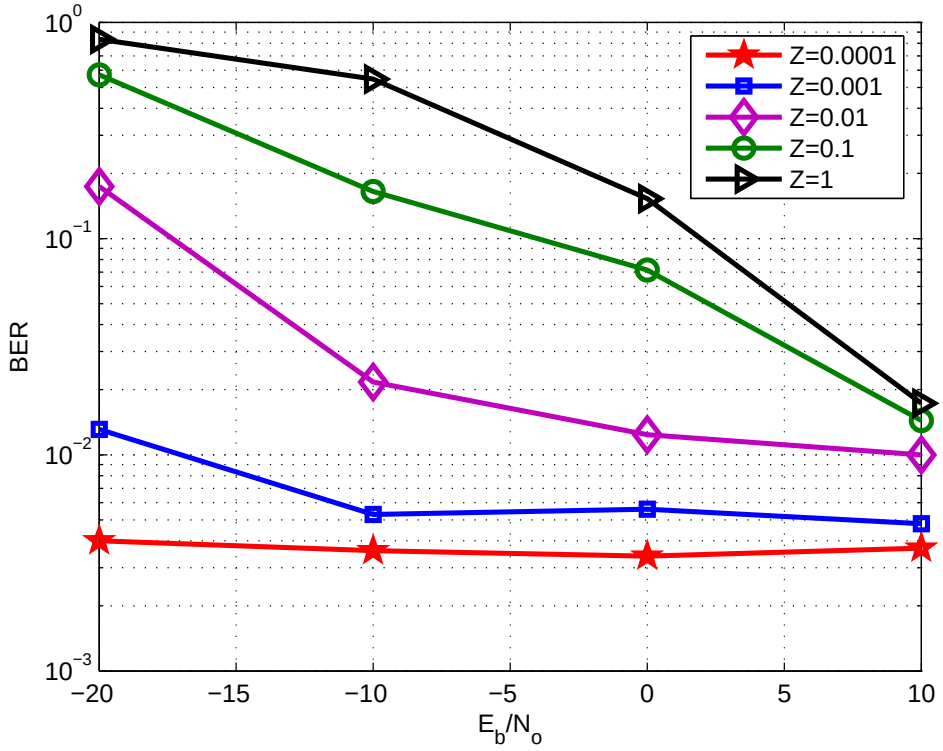

Figure 6.5. BER versus SNR for (4×4) MIMO system, impulsive noise with different values of Z and 10% channel estimation error, same variance at each receive antenna,

$$v_1 = v_2 = ... = v_N.$$

In summary, this section shows the performance of VBLAST under impulsive noise and channel estimation error. The noise model is characterized by X and Z, and it has different effects on the system. The effect of this noise at equal variance case $v_1 = v_2 = \ldots = v_{N_R}$ is lower than that at (v_p, $p = 1, 2, ..., N_R$) are i.i.d random variables. It was shown in [40] that PDC is robust to the impulsive noise, and a future study would do well to analyze this technique in the VBLAST algorithm.

6.2. Performance of MIMO CDMA Detectors for Various Channel Conditions

In this section, we show the simulation results for the proposed robust detection algorithms. We based on the STDD, RSTDD and RSIC. The following simulation parameters are used:

- Monte Carlo simulation with 10^6 bit transmissions, 4 bits each frame.
- Impulsive noise type (parameterized by ϵ and κ).
- BPSK and Rayleigh-fading MIMO channel.
- The SNR is before the channel combining.
- Perfect channel knowledge at the receiver is assumed.
- The delay error is less than one chip duration and has a Gaussian distribution with standard deviation, $\sigma = 0.1T_c$.
- Antenna configuration is $N_T \times N_R$.

Figure 6.6 depicts the performance of STDD, RSTDD and RSIC detectors under AWGN channel with different time delay estimation errors. The RSTDD outperforms the STDD by 5dB at BER of 10^{-2}, the STDD error floors at 15dB, where RSTDD achieves this output at 10dB. RSIC outperforms both detectors. Increasing the delay deviation error to 0.5 does not heavily deteriorate RSIC's performance. RSIC with 0.1 timing delay error achieves the STDD at perfect time delay estimation. The antenna setting is 2×2 for all Figures in this section.

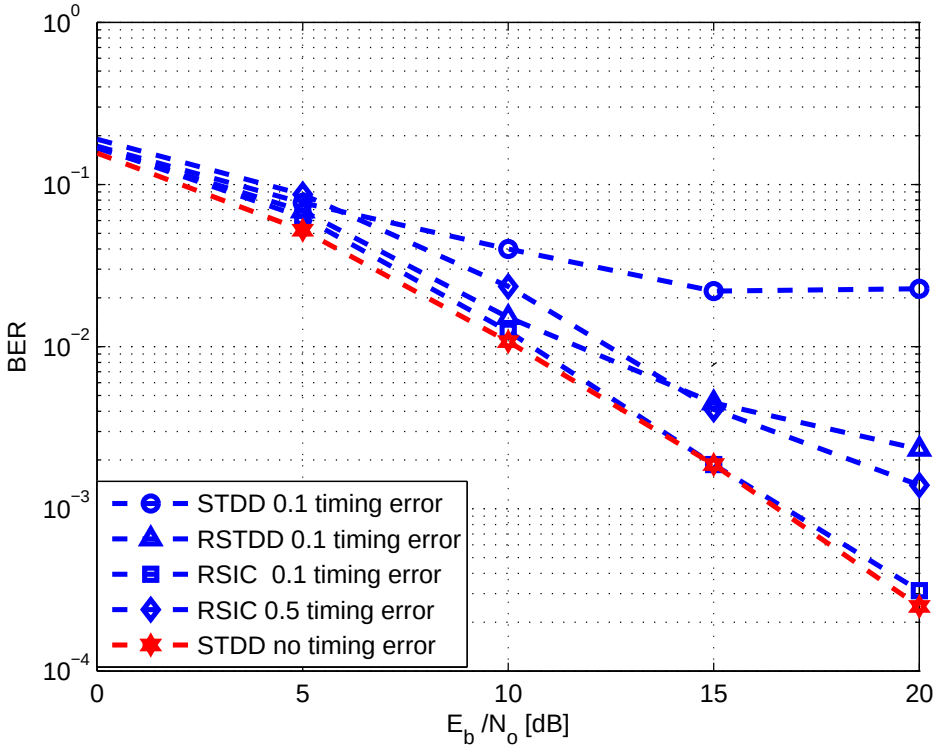

Figure 6.6. BER Performance, 2×2 MIMO CDMA system, $K = 5$ users, AWGN channel, 0.1, and 0.5 timing deviation error, near/far ratio=20dB.

The above results assume the perfect estimation of the channel coefficients. Figure 6.7 includes some channel estimation errors, where time delay deviation error is 0.1. The RSTDD gives the same performance of STDD and there is no BER enhancement achieved by this detector at this condition. RSIC continues to correctly detect the data but it needs higher SNR to succeed. Error free channel estimation RSIC performs 10^{-4} BER at 20dB while we need 10 more dB to get this performance with 0.05 channel estimation deviation error. At 0.1 channel estimation error the RSIC detector will error floor at 25dB.

Figure 6.8 shows the performance of the proposed detector which is robust to channel estimation errors in near/far case. The proposed detector achieves BER of 10^{-3} at

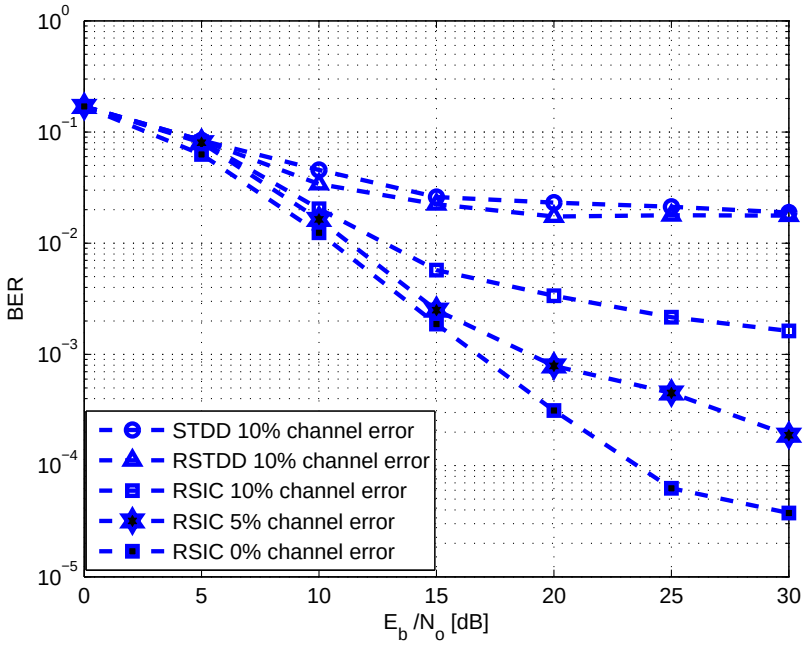

Figure 6.7. BER Performance, 2×2 MIMO CDMA system, $K = 5$ users, AWGN with different channel estimation errors, near/far ratio=20dB.

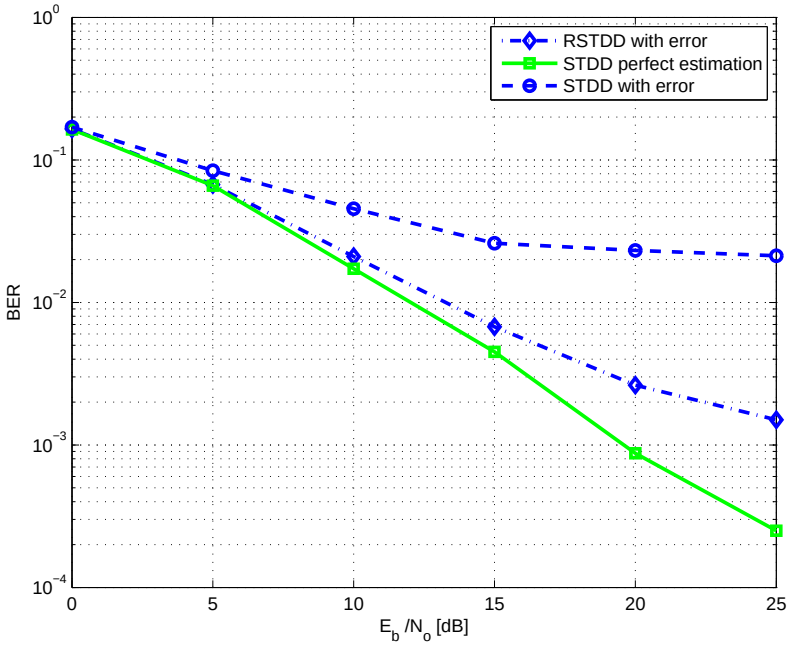

Figure 6.8. BER Performance, 2×2 MIMO CDMA system, STDD, $K = 5$ users, AWGN with 0.15 channel estimation error, near/far ratio=20dB.

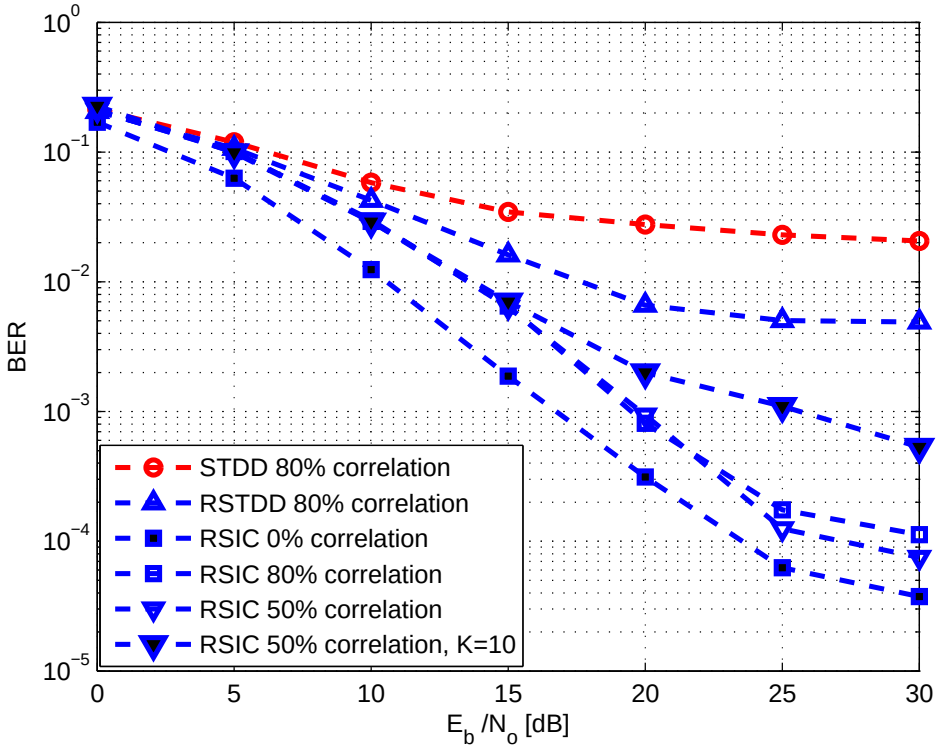

Figure 6.9. BER Performance, 2×2 MIMO CDMA system, $K = 5$ users, AWGN with partially correlated channel coefficients, near/far ratio=20dB.

20dB, the conventional STDD performs 10^{-2} at this SNR value, where no timing error problems exist.

Correlated channels have an impact on the performance of the receivers. All of the previous channel coefficients are assumed to be identically independent distributed. Figure 6.9 shows the performance deterioration when there is correlation between the channel coefficients. This correlation is known to destroy the diversity achieved by the receive antennas in the system.

The simulation curves discussed so far assume the AWGN channel. We present the simulation results to demonstrate the performance of the decorrelating detector and

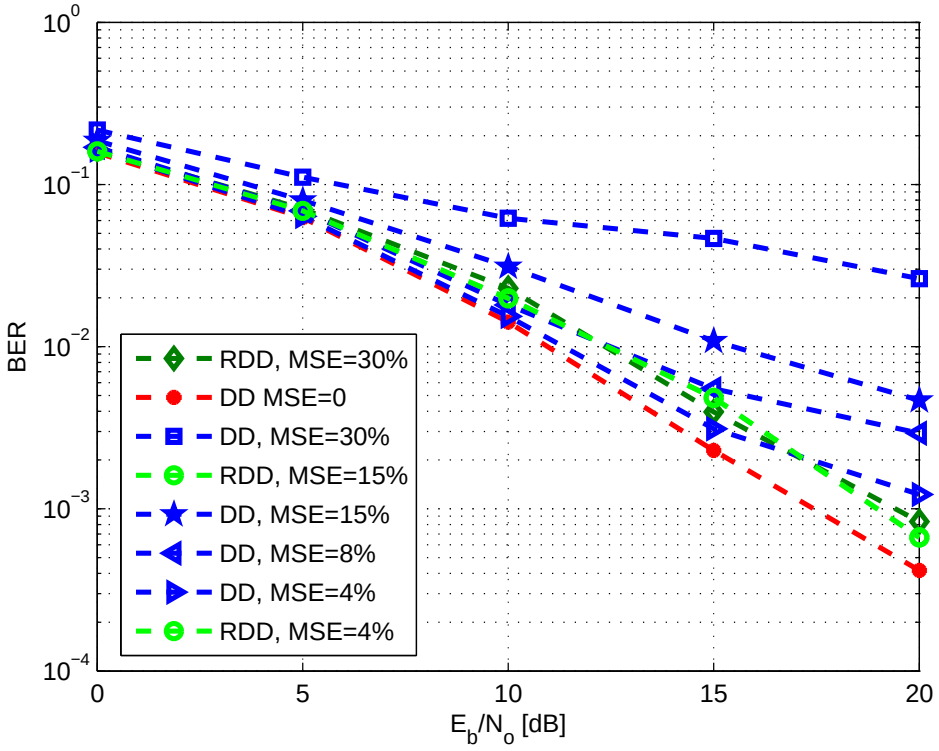

Figure 6.10. BER versus SNR for the DD and RDD, 2×2 MIMO CDMA system, with $N = 31$, $K = 6$ for various values of MSE and all users have the same power.

the proposed robust detector. We consider a MIMO CDMA system with $K = 6$ users. We first demonstrate the performance degradation of the linear multiuser decorrelating detector in different channel estimation errors. In [60], the channel coefficient mean square error is defined as:

$$MSE = E\{|c_{n,p} - \hat{c}_{n,p}|^2\}, \tag{6.1}$$

where $E\{.\}$ denotes expectation.

Figure 6.10 depicts the performance of the decorrelating detector and the robust detector for different channel estimation errors. A curve with perfect channel estimation is

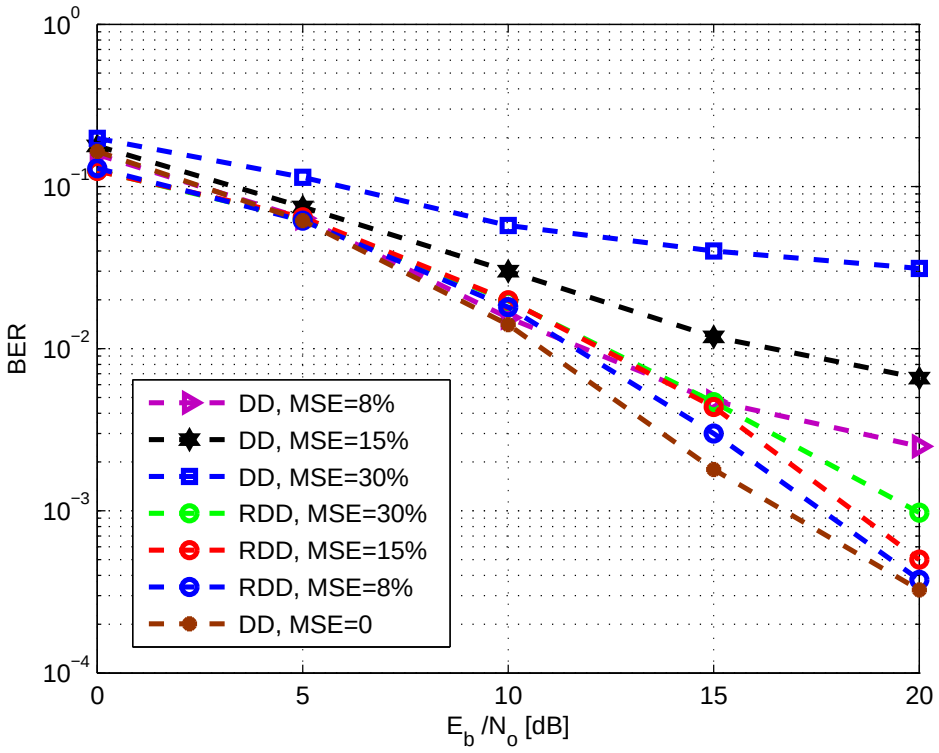

Figure 6.11. BER versus SNR for the DD and the RDD in impulsive noise, 2×2 MIMO CDMA system, with $N = 31$, $K = 6$, $\epsilon = 0.1$, $\kappa = 1000$ for various values of MSE and all users have the same power.

included as a reference. We plot the average bit error rate versus the signal-to-noise ratio under perfect power control. At $MSE = 30\%$, the DD error approximately saturates at 15dB and the RDD outperforms the DD by 10dB at BER $\approx 3 \times 10^{-2}$. For lower channel errors (15% and 8%), the RDD continues to outperform the DD significantly, and it approaches the performance of the ideal (perfect channel estimation) case.

Figure 6.11 shows the performance of the detectors under the impulsive noise channel, where the impulsive channel parameters are $\epsilon = 0.1$, $\kappa = 1000$. This represents a severely impulsive channel. We show the performance of the system where the threshold value μ for the robust non-linearity is adjusted to minimize the BER.

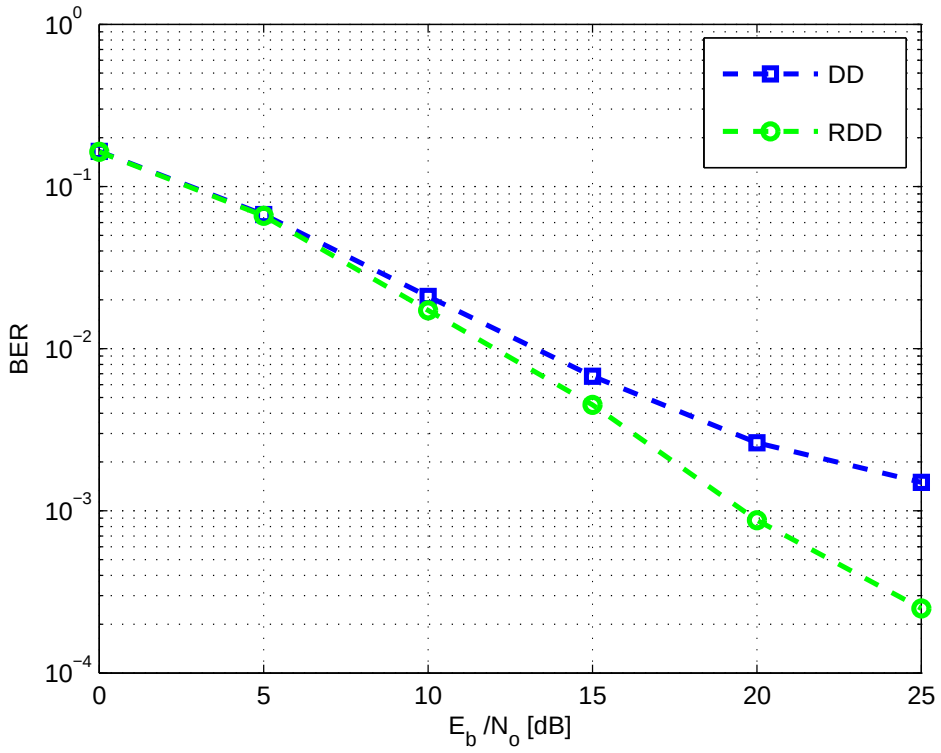

Figure 6.12. BER versus SNR of user 1 for the DD and the RDD, 2×2 MIMO CDMA system, with $N = 31$, $K = 6$, $MSE = 4\%$. The power is geometrically distributed.

At $MSE = 8\%$, the RDD outperforms the DD by 5dB, which is due to the reduced outliers of the impulsive noise process.

The next set of simulations demonstrate the performance gains achieved by the robust decorrelating detector over the linear decorrelator in a near/far scenario. The channel error is set at $MSE = 4\%$, and the near/far ratio is defined as the power ratio of the strongest interferer to that of user 1. In this case, the second user is 2dB above the first user, the third user is 2dB above the second one, and so on, so the last user (user 6) is 10dB above the first one. The bit error rate of user 1 versus SNR for the two detectors is plotted in Figure 6.12. The RDD outperforms the DD by about 5dB at a BER of 2×10^{-3}.

In conclusion, this part of the thesis shows the superior performance of the RDD over the DD, for different channel estimation errors, timing errors, noise distribution and at near/far scenario. RDD compensates the fading coefficient approximation errors by modifying the channel matrix in the process. Manipulating and modifying the spreading matrix negates the timing errors. Eventually, it goes over the impulsive components of the noise and trims them by using a clipper to cut down the impulsive consequences. The suggested RDD could possibly be utilized to enhance system capacity, particularly in unfavourable channel situations which are inherent in mobile channel.

6.3. MRC and PDC SIC Robust Detector

In this section we show the performance and analytical results. The simulations show the performance for adverse conditions, and under near/far case. The spreading Gold code length is $N = 31$. We assume synchronous CDMA transmission and ideal channel knowledge at the receiver. We denote the MRC SIC by MSIC, and the PDC SIC by PSIC in the simulation Figures. The following simulation parameters are used:

- Monte Carlo simulation with 10^6 bit transmissions, 4 bits each frame.
- Impulsive noise type (parameterized by $X = 0.1$ and Z).
- BPSK and Rayleigh-fading MIMO channel.
- The SNR is before the channel combining.
- Perfect channel knowledge at the receiver is assumed.
- No timing mismatch or channel errors in the system.
- Antenna configuration is $1 \times N_R$ (Diversity reception).

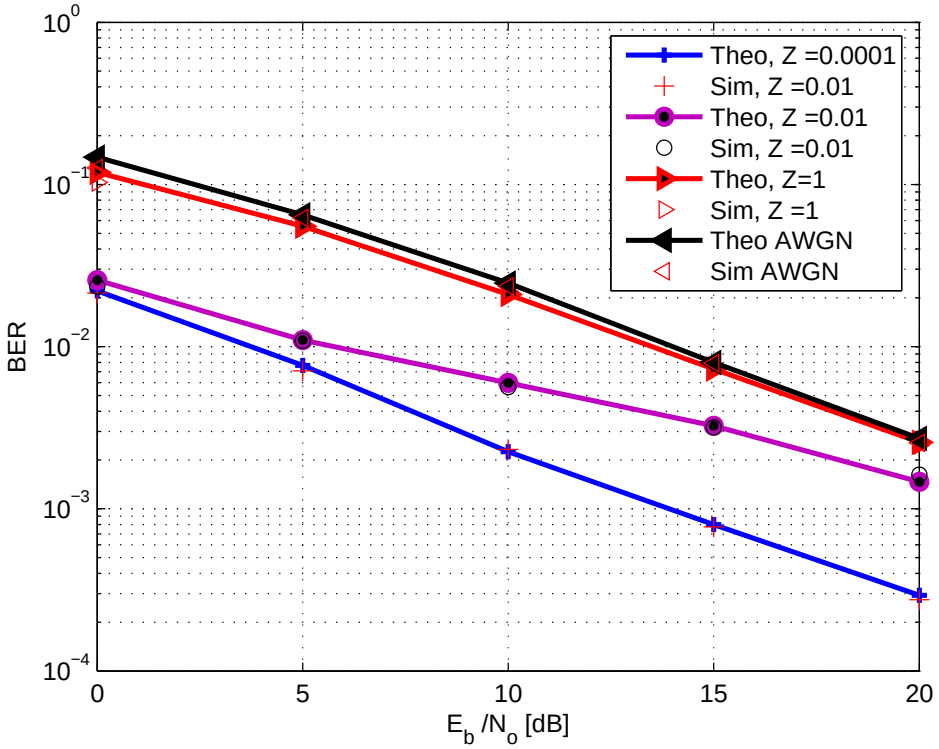

Figure 6.13. BER versus SNR for (1×1) CDMA system (analytical and simulations), $N = 31$, $K = 15$. Different values of Z and AWGN.

Figure 6.13 depicts the BER versus SNR performance for SISO system, where only MSIC is performance is simulated. The performance is shown for 15 users and all users' power are equal. The simulation curves validate the analytical ones. The BER curve for AWGN channel is also shown as a reference. The ratio of the background Gaussian noise to the impulsive one is $X = 0.1$ for all the Figures in this section. Different noise parameters are used, near Gaussian channel $Z = 1$, and highly impulsive channel $Z = 0.0001$ are used.

Figure 6.14 shows the BER versus SNR performance for a 1×3 and MSIC and PDC detection methods are used. Equal variance at each receiving antenna is assumed. For 1×3 system, the MSIC outperforms the PSIC detector. Obviously higher values

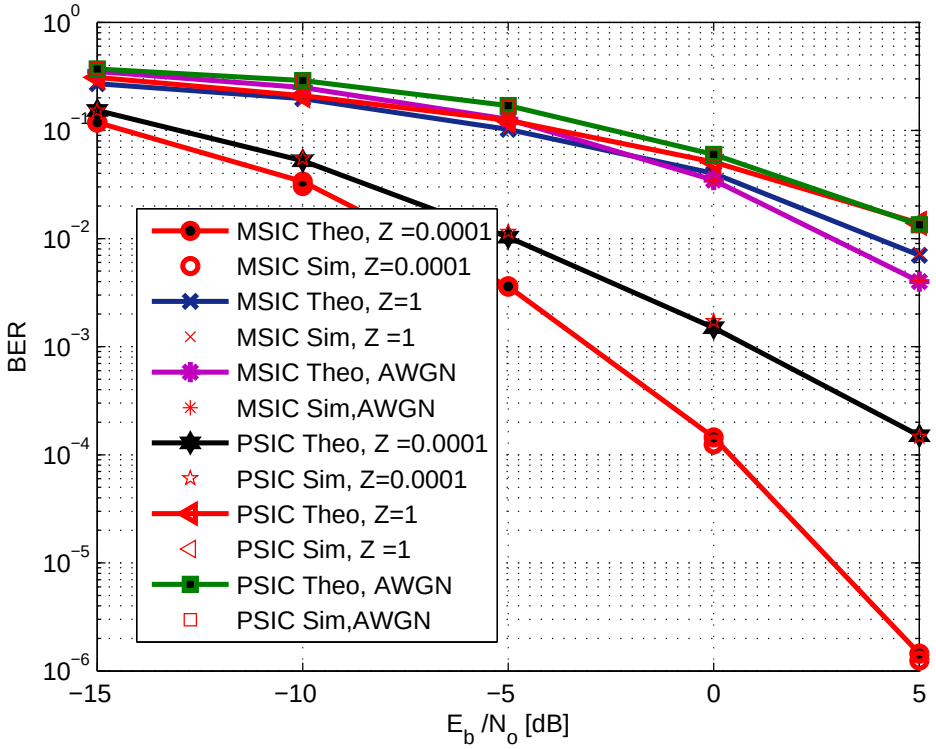

Figure 6.14. BER versus SNR for (1×3) CDMA system (analytical and simulations), $N = 31$, $K = 15$. Different values of Z and AWGN. Equal variances.

of N_R improve the BER system performance. For 1×3 system, the MSIC outperforms the PSIC detector, later we demonstrate when PSIC is better than MSIC.

Figure 6.15 displays the BER versus SNR simulation curves and MSIC analytical upper bound for a 1×2 system (i.i.d variances). In this case, the MSIC outperforms the PSIC. The bounds will serve as an indicator for the worst BER. Figure 6.16 shows the BER versus SNR simulation curves and PSIC analytical bound for a 1×3 system (i.i.d variances). The bounds are plotted, hence we need tedious derivations for getting the exact expression for the BER at i.i.d variances. The overall BER is improved due to diversity order increasing and the MSIC outperforms the PSIC.

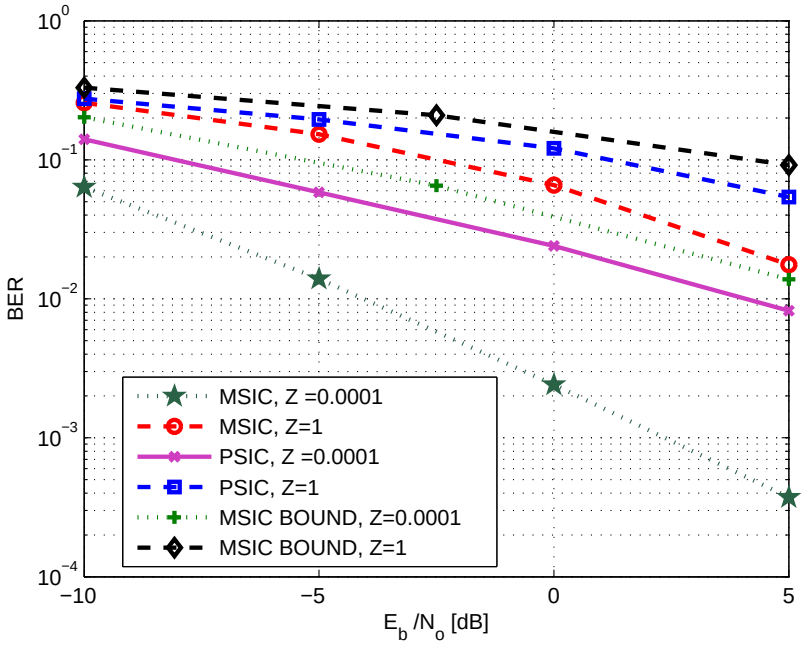

Figure 6.15. BER versus SNR for (1×2) CDMA system using MSIC and PSIC (analytical bounds and simulations), $N = 31$, $K = 15$. Different values of Z. Variances are i.i.d.

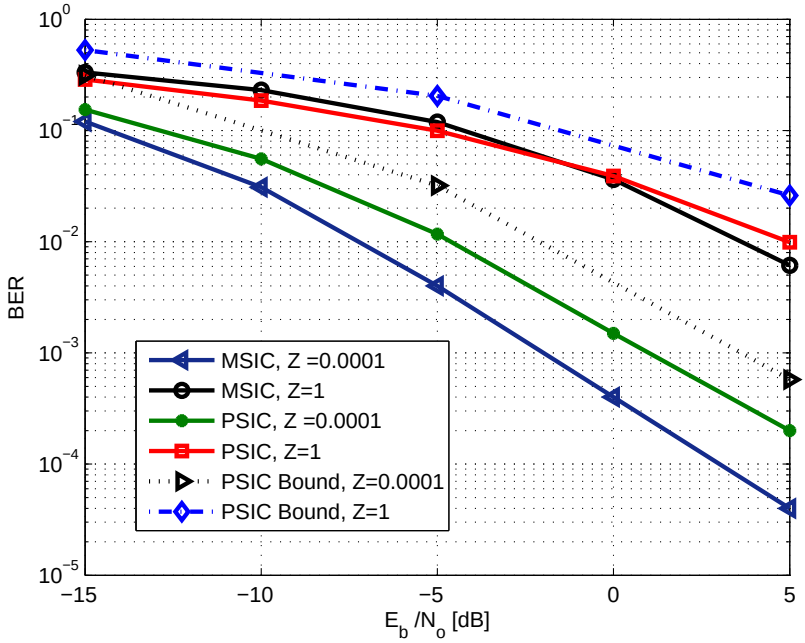

Figure 6.16. BER versus SNR for (1×3) CDMA system using MSIC and PSIC (analytical bounds and simulations), $N = 31$, $K = 15$. Different values of Z. Variances are i.i.d.

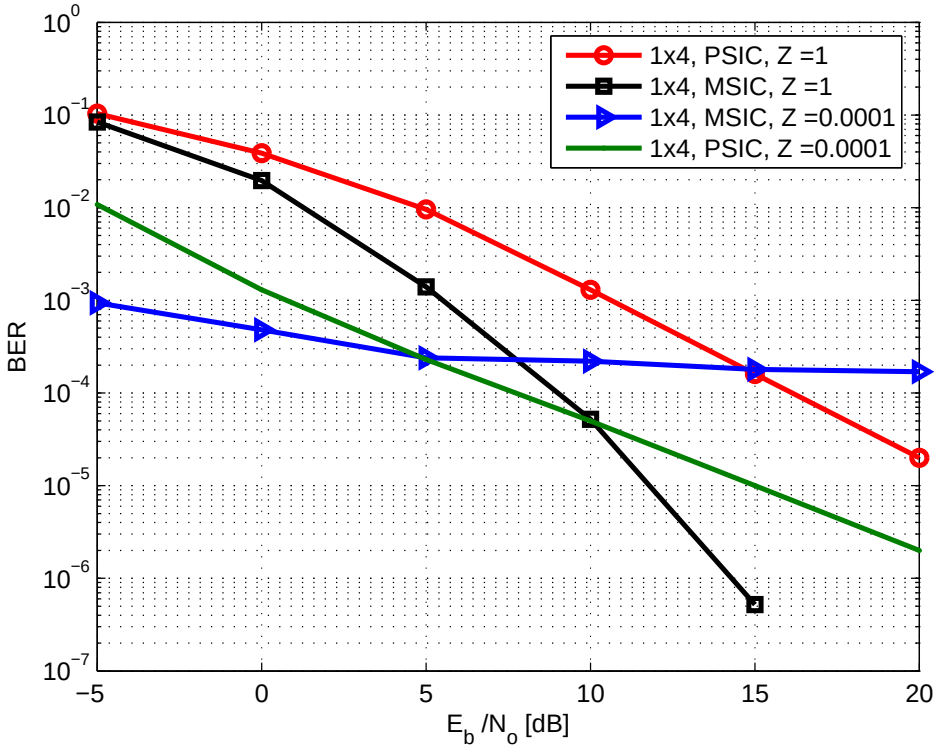

Figure 6.17. BER versus SNR for (1×4) CDMA system using MSIC and PSIC (simulations), $N = 31$, $K = 15$. Different values of Z. Variances are i.i.d.

Figure 6.17 demonstrates the BER versus SNR simulation results for a 1×4 system (i.i.d variances). Now the outperforming technique will not be the MSIC as in the previous Figures, the PSIC outperforms the MSIC, particularly, when increasing the SNR values. Figure 6.18 shows the BER versus SNR simulations and PSIC bound for a 1×5 system (i.i.d variances). We again notice the superior performance of the PSIC in this Figure. This gives an insight to choose the PSIC detection as the robust detection when having i.i.d variances. The MSIC is error flooring after -4dB and show negligible improvement in the higher SNR range. On the other hand, The PSIC gives a substantial performance over the MSIC at high SNR values.

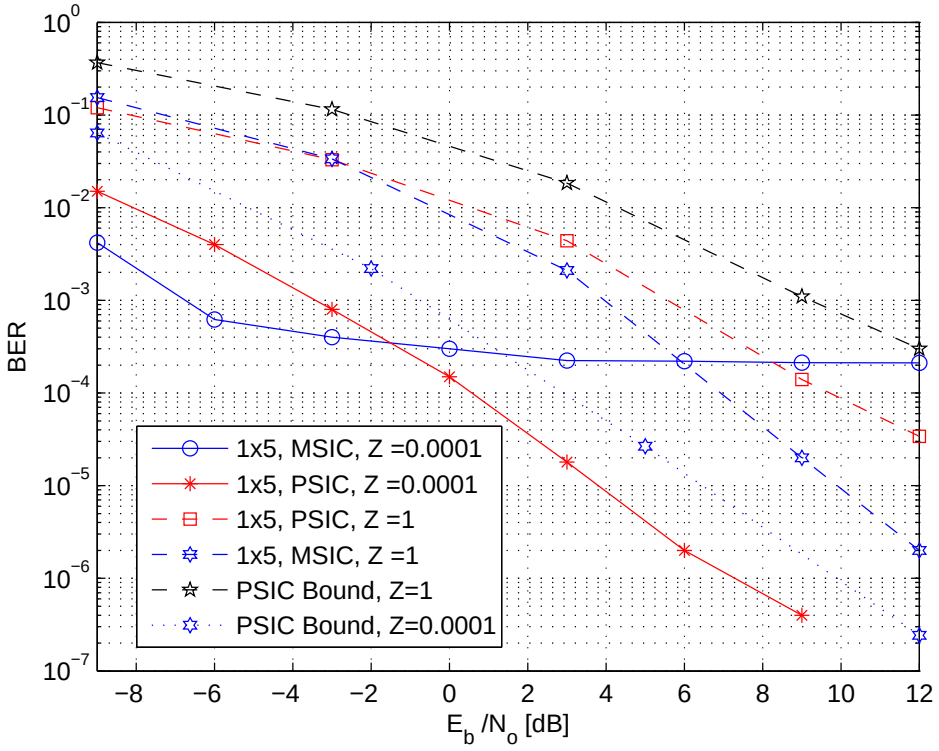

Figure 6.18. BER versus SNR for (1×5) CDMA system using MSIC and PSIC (analytical bounds and simulations), $N = 31$, $K = 15$, Different values of Z. Variances are i.i.d.

The following Conclusion can be drawn, the PSIC outperforms the MSIC detector when $N_R \geq 4$ at high impulsive noise case, i.e when $Z = 0.0001$, otherwise, the MSIC gives a substantial performance over the PSIC when $N_R < 4$, or when the channel is near Gaussian $Z = 1$ for any value of N_R.

Finally, we depict the performance of both detectors in a near/far scenario in Figures 6.19 and 6.20, for a 1×2 and a 1×5 system respectively. The near/far effect is defined to be the ratio of the maximum power to the weakest user power (desired user), and set to be 20dB, the number of users is 5 and all the other users are 20dB above the weakest user. The simulations are done for 1×2 and 1×5 systems, for different Z values and the BER curve is plotted for the desired user.

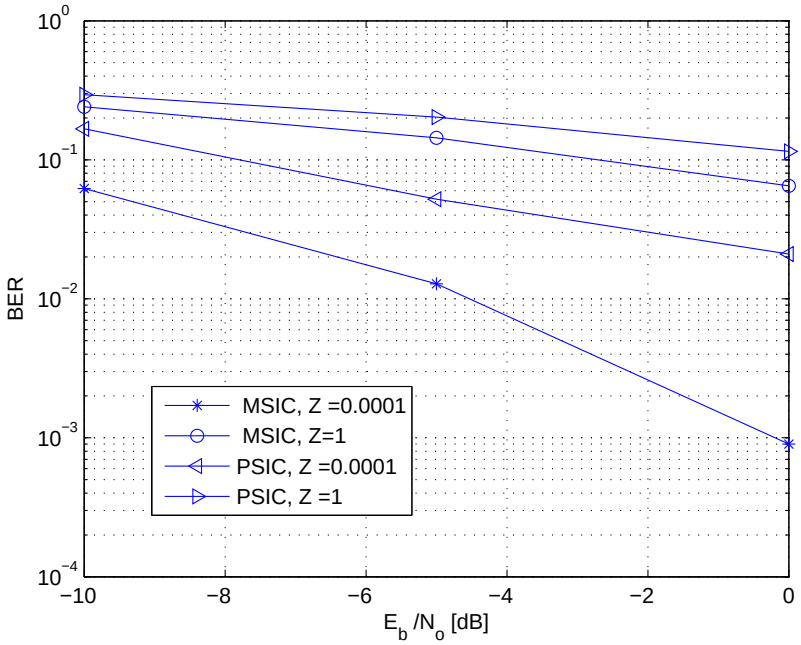

Figure 6.19. BER versus SNR for (1×2) CDMA system under 20dB near/far scenario, using MSIC and PSIC, (BER of the desired user), $N = 31$, $K = 5$. Different values of Z. Equal variances.

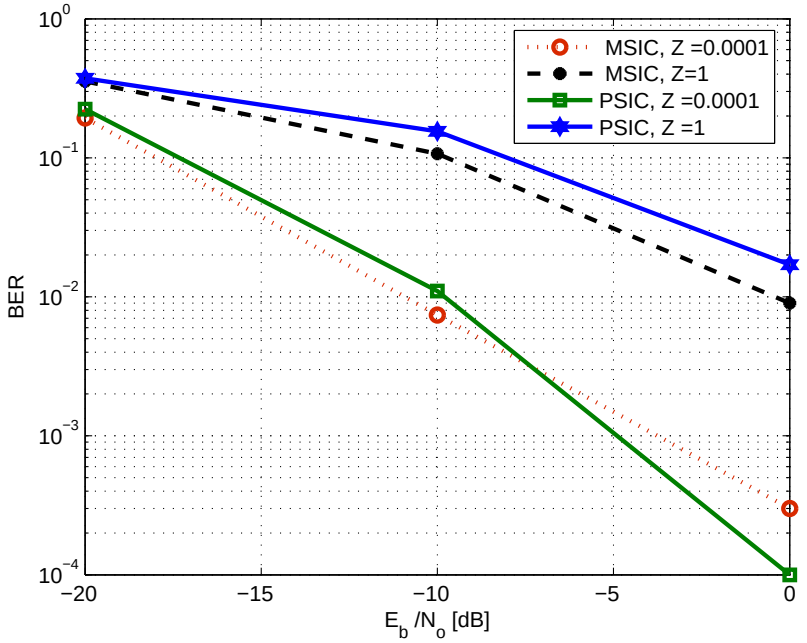

Figure 6.20. BER versus SNR for (1×5) CDMA system under 20dB near/far scenario, using MSIC and PSIC, (BER of the desired user), $N = 31$, $K = 5$. Different values of Z. Variances are i.i.d.

We expect that the MSIC will outperform the PSIC for a 1×2, and the PSIC will overtake the MSIC for a 1×5. This was concluded form the previous simulations. Figures 6.19 and 6.20 demonstrate the BER performance, on observation of these Figures, our expectations are confirmed.

In summary, throughout this section, the performance of low complexity SIC detector under impulsive noise is studied, two diversity reception methods were considered, namely MRC SIC and PDC SIC. The section pointed out the cases where each detector outperforms the other. We stated a clear derivations with perfect agreement of simulations. Bounds were depicted for both detectors. This part of the thesis will provide a benchmark for the study of SIC algorithm in multi antenna systems with impulsive noise. Future work may extend this research to frequency selective and multipath fading scenarios, coding systems and multicarrier communications.

6.4. DD and RDD

In this section, we show the simulation results of the DD and the proposed RDD. We depict the BER curves using simulations and analytical derivation that we derived. We also show that the propped RDD outperforms the DD in impulsive channels. The simulations are done for 10^7 bit transmissions, where the transmissions are done for 4 bit size frames ($M = 4$), $K = 5$ users, and different antenna configurations. The complex channel coefficients are assumed to be known and normalized to unity at the receiver, hence we are more interested to show the effect of the noise model. The spreading code length is $N = 31$ and all the users have the same power. The E_b/N_o is defined to be the signal-to-noise ratio at every receiving branch. Performance studies have been carried out both theoretically and experimentally. The abbreviations (Theo) and

(Sim) are used to designate theoretical and simulated curves. The following simulation parameters are used:

- Monte Carlo simulation with 10^7 bit transmissions, 4 bits each frame.
- Two Impulsive noise types (parameterized by $X = 0.1$, Z, ϵ, and κ).
- BPSK and Rayleigh-fading MIMO channel.
- The SNR is before the channel combining.
- Perfect channel knowledge at the receiver is assumed and normalized to unity at the receiving end.
- No timing mismatch or channel errors in the system.
- Antenna configuration is $1 \times N_R$ (Diversity reception).

Figure 6.21 depicts the BER versus SNR simulation and theoretical curves of the performance of the decorrelating detector, under unconstraint (fixed variance method [38]) in a 1×1 system. The constraint condition (varying ϵ and κ without keeping fixed total variance) is shown in Figure 6.22. The simulation is done for different values of ϵ and κ, and the antenna system is $N_T \times N_R = 1 \times 1$. Based on the analysis and derivations in the previous chapter, these simulations are plotted.

It is clear that the impulsive noise degrades system performance. For example, in Figure 6.22, the curve where $\epsilon = 0.01$ and $\kappa = 1000$ has a 6dB difference with the AWGN curve at a BER of 2×10^{-3}. Usually, the constraint model is used.

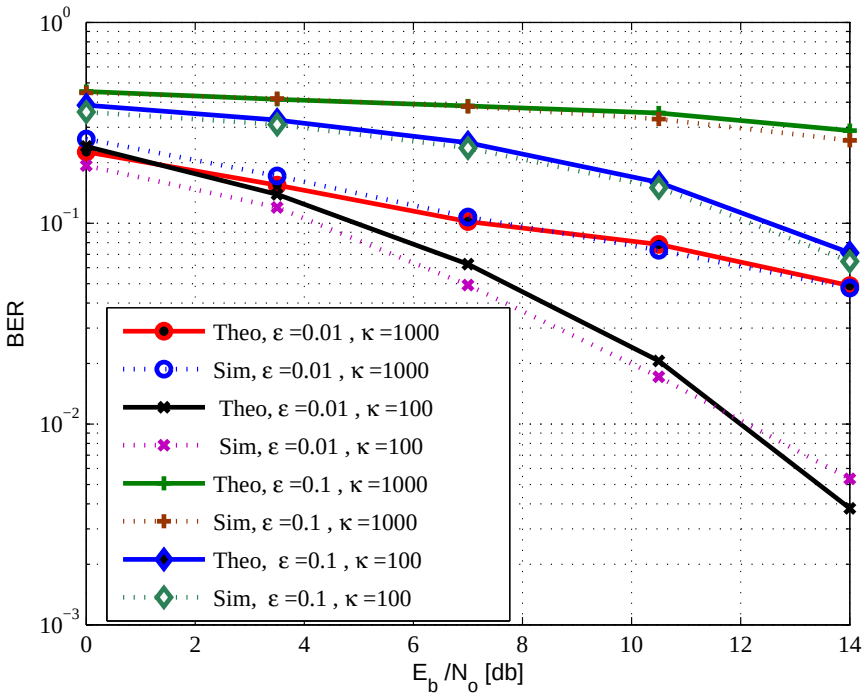

Figure 6.21. BER versus SNR for constraint (1×1) CDMA system using DD, impulsive noise with $N = 31$, $K = 5$, different values of ϵ and κ.

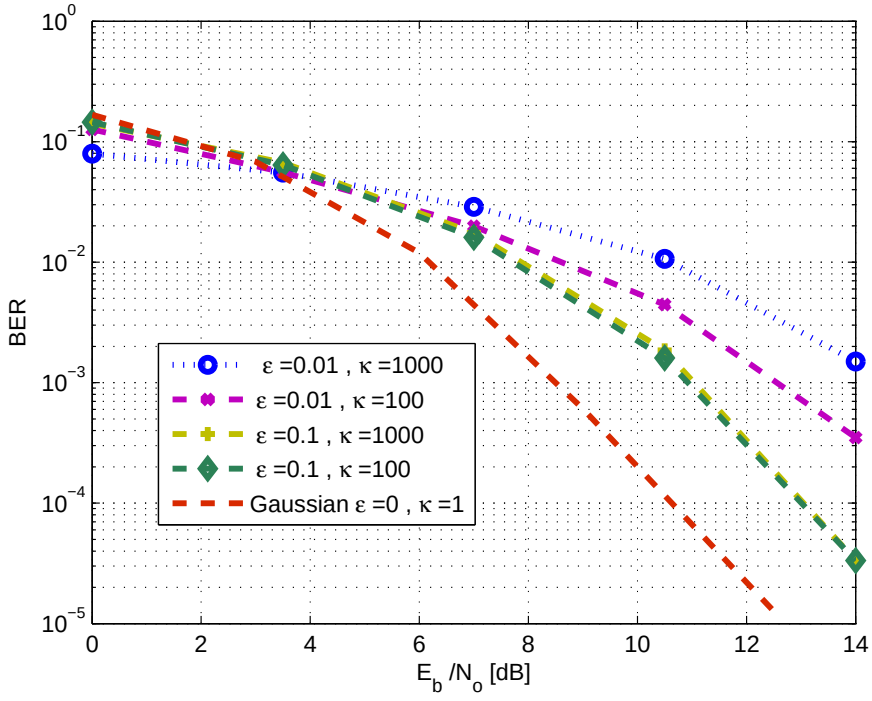

Figure 6.22. BER versus SNR for non-constraint (1×1) CDMA system using DD, impulsive noise with $N = 31$, $K = 5$, different values of ϵ and κ.

However, we provide one simulation for the non-constraint case to show its behavior as in Figure 6.21, and adopt the constraint strategy for all consequent simulations.

Next we will see the diversity effect on the system. Figure 6.23, shows the 1×2 system performance where the simulation curves do not have a large variation at different noise parameter values. Increasing the receive diversity to 1×3 system will decrease the error as Figure 6.24 depicts.

Finally, Figure 6.25 displays the fourth order receive diversity system. It shows the significant increase in the system's performance, at higher receive diversity order.

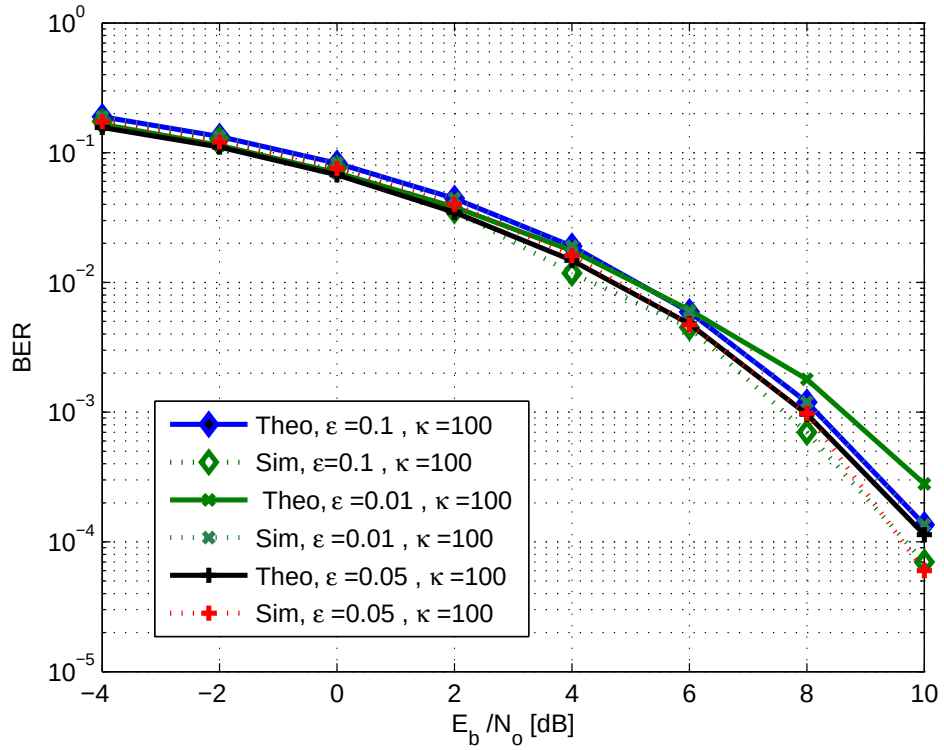

Figure 6.23. BER versus SNR for (1×2) CDMA system (theoretical and simulations) using DD, impulsive noise with $N = 31$, $K = 5$, constraint system, different values of ϵ and κ.

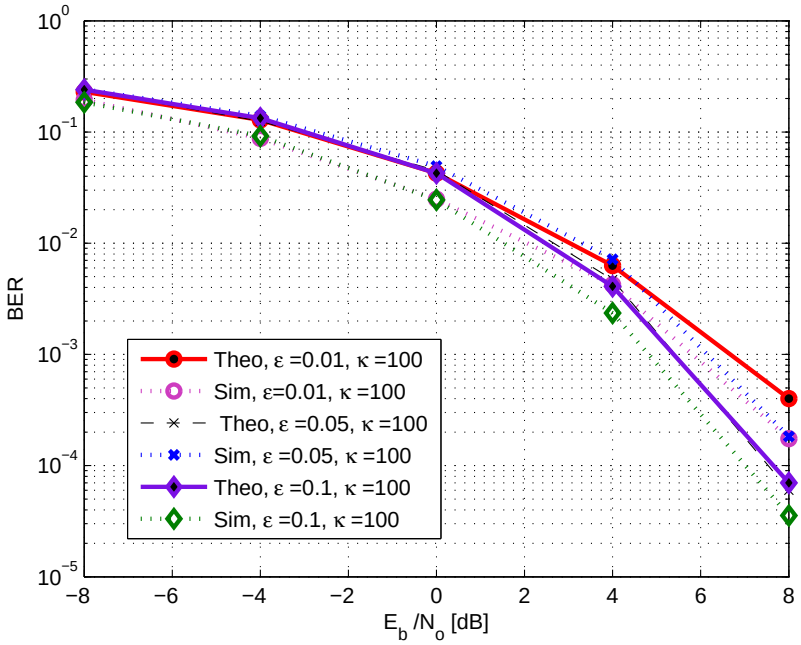

Figure 6.24. BER versus SNR for (1×3) CDMA system (theoretical and simulations) using DD, impulsive noise with $N = 31$, $K = 5$, constraint system, different values of ϵ and κ.

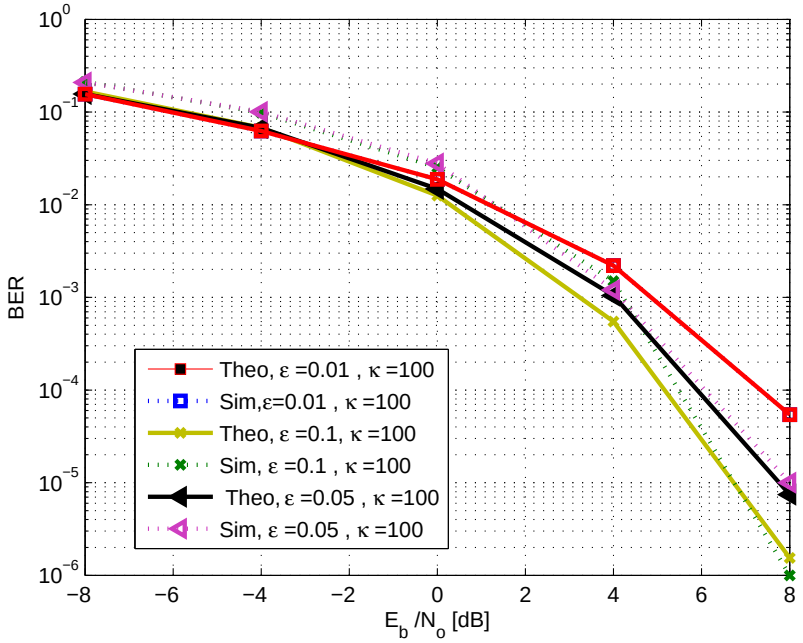

Figure 6.25. BER versus SNR for (1×4) CDMA system (theoretical and simulations) using DD, impulsive noise with $N = 31$, $K = 5$, constraint system, different values of ϵ and κ.

At high SNR the simulation curves variations begin to increase at different ϵ and κ. We should note that the SNR is defined to be the SNR at each receiving branch.

Theoretical and simulations curves may have a certain degree of difference, that is due to the sample noise variance distribution as in [38]. Asymptotically, the linear decorrelating detector performance is absolutely identified by the noise variance independent of the noise pdf. On the other hand, the noise distribution does considerably influence the finite sample performance of the decorrelating detector.

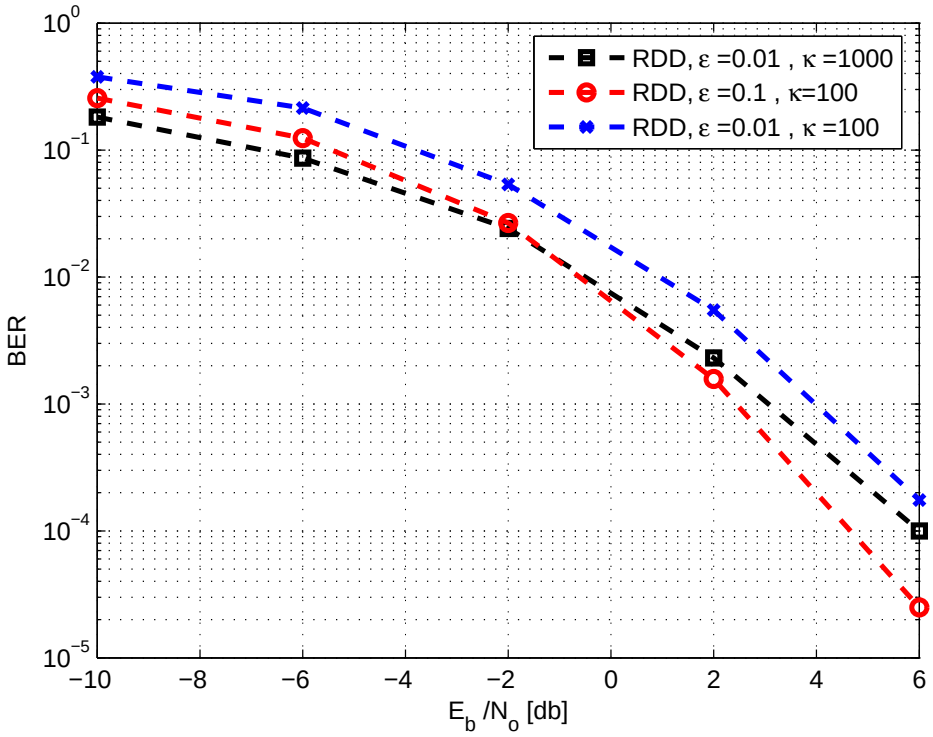

Figure 6.26. BER versus SNR for (1×4) CDMA system using RDD , impulsive noise with $N = 31$, $K = 5$, constraint system, different values of ϵ and κ.

We use a robust non-linearity at each receiving branch, and we gain a good performance, as shown in Figure 6.26. RDD outperforms DD by trimming the impulsive effects. For example, when $\epsilon = 0.01$ and $\kappa = 100$, the BER at 4 dB for the DD (no

clipping) is 2×10^{-3}, but the BER for the RDD (with clipping) is 5×10^{-4}.

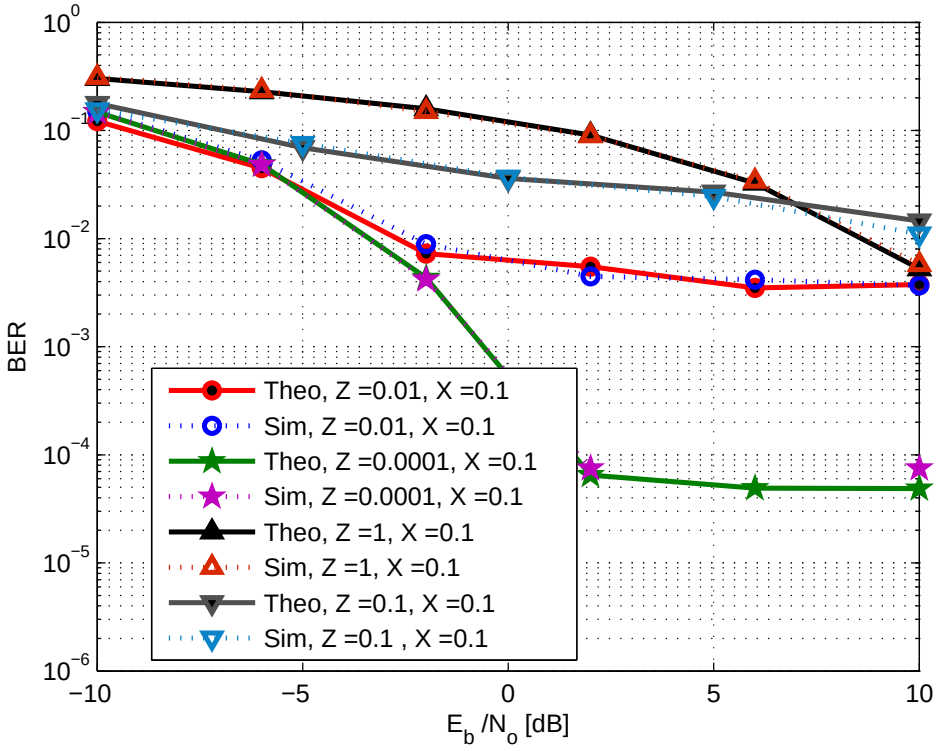

Figure 6.27. BER versus SNR for (1×1) CDMA system (theoretical and simulations) using DD , impulsive noise with $N = 31$, $K = 5$, different values of X and Z.

Now, we will discuss the performance of the CDMA system under the impulsive noise model that is parameterized by Z and X. First we discuss the 1×1 antenna system. Figure 6.27 shows the performance of the system in the near Gaussian noise case where $Z = 1$ and highly impulsive case where $Z = 0.0001$. The theoretical curves reveal the simulated results with the help of the analytical steps from the previous chapter.

In Figure 6.28, we show the performance of a 1×2 CDMA system, where MRC reception is considered. The simulation curves match the analytical ones when the single poisson random variable (v_p, $p = 1, 2, \ldots, N_R$) is assumed to be equal at all the

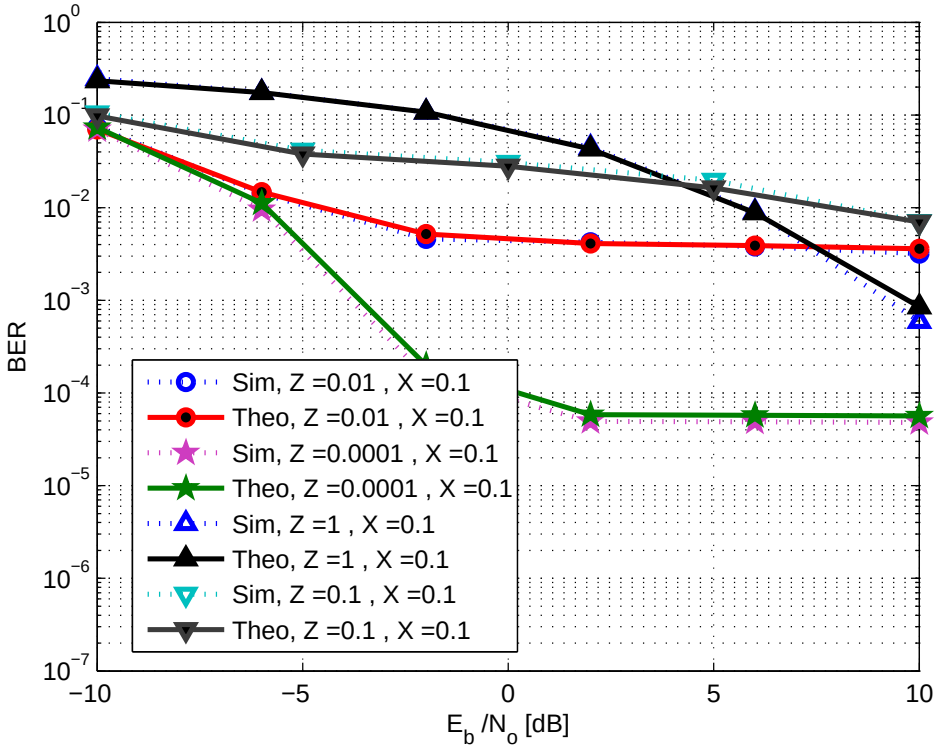

Figure 6.28. BER versus SNR for (1×2) CDMA system (theoretical and simulations) using DD , impulsive noise with $N = 31$, $K = 5$, different values of X and Z. (v_p, $p = 1, 2$) are assumed to be equal.

receiving antennas, i.e, $v_1 = v_2 = \ldots = v_{N_R}$. However, if the random variable (v_p) is different at every receiving antenna, MRC is not outperforming.

The BER changes and decreases while increasing the number of the receiving antennas due to diversity as shown in Figure 6.29. For example, for $X = 0.1$ and $Z = 1$, at a BER of 10^{-2}, it needs 5.5dB for a 1×2 system, and 4.5dB for a 1×3. When moving to different values of the noise parameters ($X = 0.1$ and $Z = 0.01$), BER of 4×10^{-2} requires 0dB for a 1×2 system, and -5dB for a 1×3. It is known that the MRC is outperforming when the noise variances are dependent. However, if the variances are i.i.d, then the PDC is a better combining scheme. This can be explained by the diversity

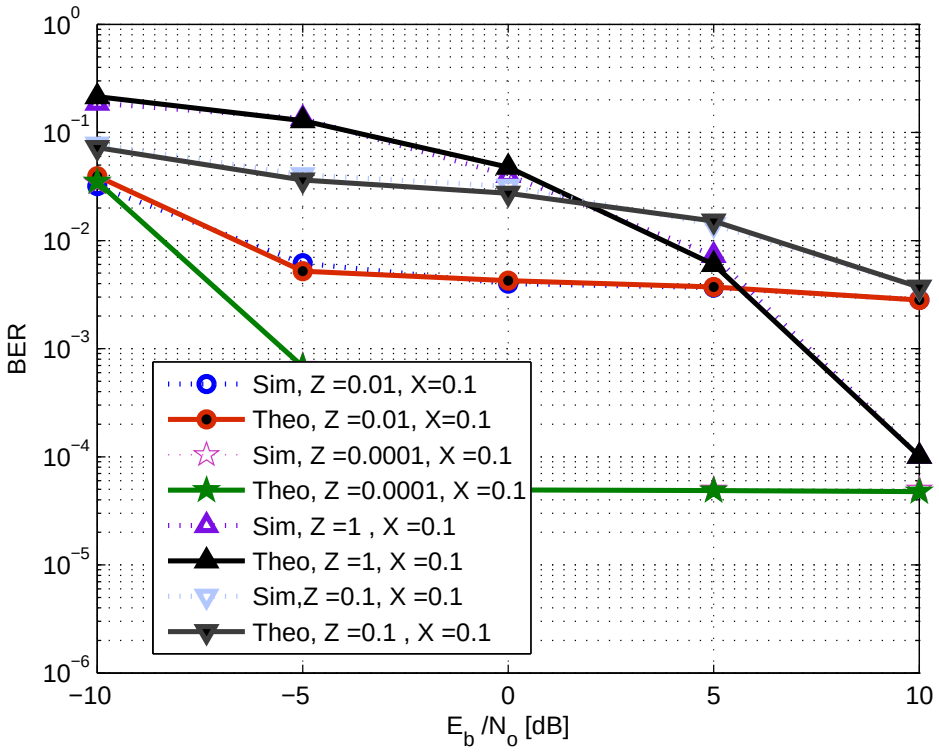

Figure 6.29. BER versus SNR for (1×3) CDMA system (theoretical and simulations) using DD , impulsive noise with $N = 31$, $K = 5$, different values of X and Z. (v_p, $p = 1, 2, 3$) are assumed to be equal.

gain. The MRC has higher diversity gain when the number of receiving branches is less than four. At that case, the PDC has less diversity gain, consequently, it has worse performance. When the number of receiving branches is getting more than four, the PDC will start to gain some diversity order, consequently, it will outperform the MRC scheme. This is verified through the simulation of Figure 6.30 which depicts the result of a 1×4 system, where the conditional variances (v_p, $p = 1, 2, ..., N_R$) are assumed to be i.i.d random variables. In this case PDC simulation shows that its more robust under this noise case. At $X = 0.1$ and $Z = 0.01$ the PDC case outperforms the MRC method by 10dB at BER of 10^{-2}. Another case where $X = 0.1$ and $Z = 0.1$ also has

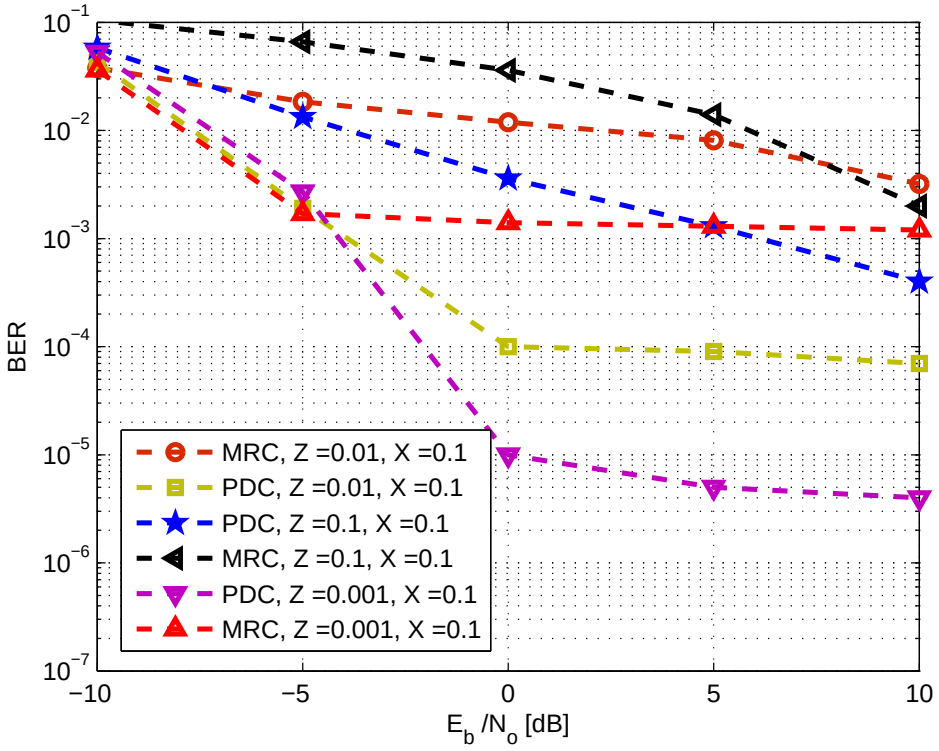

Figure 6.30. (PDC versus MRC) BER versus SNR for (1×4) CDMA system (simulations) using DD , impulsive noise with $N = 31$, $K = 5$, different values of X and Z. (v_p, $p = 1, 2, 3, 4$) are assumed to be i.i.d random variables.

10dB difference toward the PDC side. Finally, when $X = 0.1$ and $Z = 0.001$, the MRC receiving technique error floors near -5dB for a BER of 10^{-3}, and PDC gets a BER of 10^{-5} at 0dB, and decreases slowly after that point. Note that we normalized the fading coefficient in all the simulated graphs and focused on the noise effect.

Chapter 7

CONCLUSIONS AND FUTURE WORK

7.1. Conclusions

In this thesis, we investigated the performance gain of the RDD over the DD for different channel estimation errors, timing errors, noise distributions, and near/far scenarios. RDD compensates the fading coefficient approximation errors by modifying the channel matrix in the process. Manipulating and modifying the spreading matrix eliminates the timing errors, Eventually, RDD goes over the impulsive components of the noise and trims them by using a clipper to diminish the impulsive consequences. This new RDD could possibly be applied to enhance system capacity, particularly in unfavorable channel situations which are inherent in mobile channels. We also discussed the performance of V-BLAST under impulsive noise and channel estimation error. The noise model characterized by X and Z, and it has a different effect on the system, the effect of this noise at equal variance case $v_1 = v_2 = \ldots = v_{N_R}$ is lower than that at (v_p, $p = 1, 2, ..., N_R$) are i.i.d random variables.

We proposed a robust low complexity SIC detector under impulsive noise. We consider two diversity reception methods, namely MRC SIC, and PDC SIC. The work points the cases where each detector is outperforming the other one. We derived novel analytical results and verified them by simulations. Performance bounds were also derived and

depicted for both detectors. The performance of the system under power imbalance is also shown. The research done provides a detailed study of a SIC algorithm in multi antenna systems with impulsive noise. We found that each detector outperforms the other depending on certain conditions such as; the strength of the impulsive noise, the noise variance at each receiving antenna (i.i.d or not), and the number of receiving antennas (N_R). We conclude that:

- MSIC outperforms the PSIC when the noise variance is equal at each receiving branch regardless of the value of Z or N_R.
- If the noise variance at each receiving branch is i.i.d, then we observe these cases:
    1. MSIC outperforms the PSIC for near gaussian case (i.e $Z = 1$), regardless of the value of N_R.
    2. MSIC outperforms PSIC for highly impulsive case (i.e $Z = 0.0001$) if $N_R \leq 3$.
    3. PSIC outperforms MSIC for highly impulsive case if $N_R \geq 4$.

We also investigated the performance of the decorrelating detector under impulsive noise using two noise models, and analyzed them discretely. The first noise model is two densities gaussian mixture model parameterized by ϵ and κ. The effect of this noise was investigated and a RDD is employed to overcome the impulsive effects. The second noise model has infinite expansion of gaussian densities, and characterized by X and Z, it has a different effect on the system. MRC is a technique to get low BER

(at equal variance case $v_1 = v_2 = \ldots = v_{N_R}$), and the robust technique for this case is PDC. We realized from the simulations that PDC performs quite well when the variance at each receive antenna is not equal, (v_p, $p = 1, 2, ..., N_R$) but assumed to be i.i.d random variable.

We have discussed the complexity issues in MSIC and PSIC. The complexity of these detectors is a very important aspect, hence we require fast processing communication devices that handle the high data rate transmission. We can also conclude that MSIC is a good downlink choice, because the antenna spacing would be close, and MSIC outperforms in these conditions. On the other hand, we should use the PSIC for the uplink side, hence the antenna spacing would be high enough that the noise variances are i.i.d and the PSIC is outperforming under this scenario.

7.2. Future Work

Orthogonal frequency-division multiplexing is a common method for high-data-rate communication. OFDM may be bundled with multiple antennas at both the access point and the mobile terminal to improve diversity gain and/or enhance system capacity. Indeed, it is a standard for the recent MIMO CDMA. Future work would continue this research to investigate the performance of MIMO OFDM CDMA system, especially, the peak to average power ratio problem, which is common in OFDM system, these peaks together with the impulsive peaks could be a fascinating research area.

Another key challenge facing MIMO technology in 3G cellular networks is the sensitivity of MIMO receivers to interference. Since cellular systems are inherently interference-limited. In addition to inter antenna and intra antenna interference, we

have the MAI in CDMA, and CDMA capacity is interference limited as well. Studying and investigating the interference in MIMO CDMA from all the sources (CDMA, and MIMO antennas) would also be a good future work. It is also important to investigate the Wide-bande CDMA with MIMO system, hence it is closer to the real and practical scenarios. The research could be also extended to:

- Frequency selective and multipath fading channels.
- Coding systems and multicarrier communications.
- Analysis of channel estimation errors on MIMO OFDM CDMA.

REFERENCES

[1] T. S. Rappaport, A. Annamalai, R. M. Buehrer and W. H. Tranter, "Wireless communications: Past events and a future perspective," *IEEE Communications Magazine*, vol. 40, no. 5, pp. 148-161, May 2002.

[2] K. S. Gilhousen, I. M. Jacobs, R. Padovani, A. J. Viterbi, L. A. Weaver, Jr and C. E. Wheatley III, "On the capacity of a cellular CDMA system," *IEEE Transactions on Vehicular Technology*, vol. 40, no. 2, pp. 303-311, May 1991.

[3] S. Verdu, "Optimum sequence detection of asynchronous multiple-access Communications," *in Proceedings of the 1983 IEEE International Symposium Information Theory*, pp. 80, St. Jovite, Canada, September 1983.

[4] S. Verdu, "Minimum probability of error for asynchronous Gaussian multiple-access channels," *IEEE Transactions on Information Theory*, vol. 32, pp. 85-96, January 1986.

[5] H. Abuhilal, A. Hocanin, and H. Bilgekul, "Robust MIMO-CDMA decorrelating detector," *IEEE International Conference on Signal Processing and Communications (ICSPC)*, pp. 732-735, November 2007.

[6] H. Abuhilal, A. Hocanin, and H. Bilgekul, "Performance of RSIC detector for MIMO CDMA signals with time mismatch," *IEEE Sinyal Isleme ve Uygulamalari Kurultayi (SIU'2007)*, Turkey, June 2007.

[7] H. Abuhilal, A. Hocanin, and H. Bilgekul, "Performance of V-BLAST In impulsive noise," *IEEE Sinyal Isleme ve Uygulamalari Kurultayi (SSIU' 08)*, Turkey, June 2008.

[8] H. Abuhilal, A. Hocanin and H. Bilgekul, "Successive interference cancellation for a CDMA system with diversity reception in non-gaussian noise," *International Journal of Communication Systems (IJCS), Wiley*. OCT 2011.

[9] Z. Zvonar, "Multiuser detection in asynchronous CDMA frequency-selective fading channels," *Wireless Personal Communications*, vol. 2, pp. 373-392, 1996.

[10] Z. Zvonar and D. Brady, "Linear multipath-decorrelating receivers for CDMA frequency-selective fading channel," *IEEE Transactions on Communications*, vol. 44, pp. 650-653, 1996.

[11] A. J. Viterbi, "The orthogonal-random waveform dichotomy for digital mobile personal communications," *IEEE Personal Communication*, vol. 1, no. 1, pp. 18-24, 1994.

[12] R. L. Pickholtz, L. B. Milstein and D. L. Schilling, "Spread spectrum for mobile communications," *IEEE Transactions on Vehicular Technology*, vol. 40, no. 2, pp. 313-22, May 1991.

[13] S. Verdu, *Multiuser detection*. Cambridge, U.K.: Cambridge University Press, 1998.

[14] V. K. Garg, K. Smolik and J. E. Wilkes, *Applications of Code-Division Multiple Access (CDMA) in Wireless Personal Communications*, Upper Saddle River, NJ: Prentice Hall, 1996.

[15] J. G. Proakis, *Digital Communications*, 2nd ed., New York, McGraw-Hill, 1989.

[16] M. K. Varanasi and B. Aazhang, "Multistage detection in asynchronous code division multiple-access communications," *IEEE Transactions on Communications*, vol. 38, no. 4, pp. 509-519, April 1990.

[17] Alexandra Duel-Hallen, "Decorrelating decision-feedback multiuser detector for synchronous code-division multiple-access channel," *IEEE Transactions on Communications*, vol. 41, no. 2, pp. 285-290. February 1993.

[18] Alexandra Duel-Hallen, "A family of multiuser decision-feedback detectors for asynchronous code-division multiple-access channels," *IEEE Transactions on Communications*, vol. 43, no. 2, pp. 421-427. February 1995.

[19] D. Koulakiotis and A. H. Aghvami, "Comparative study of interference cancellation schemes in multi-user detection, CDMA Techniques and applications for third generation mobile systems" (Digest No.: 1997/129), *IEE Colloquium on.,*, pp. 101-107, May 1997.

[20] V. Wijk F. Janssen GMJ and R. Prasad, "Groupwise successive interference cancellation in a DS/CDMA system," *In Proceedings of the IEEE International Symposium on Personal, Indoor, and Mobile Radio Communications (PIMRC' 95)*, Toronto, Canada, vol. 2, pp. 742-746, 1995.

[21] S. Verdu, "Optimum multiuser asymptotic efficiency," *IEEE Transactions on Communications*, vol. 34, no. 9, pp. 890-897, September 1986.

[22] V. Tarokh, H. Jafarkhani and A. R. Calderbank, "Space-time block coding for wireless communications: Performance results," *IEEE Journal on Selected Areas in Communications*, vol. 17, pp. 451-460, March 1999.

[23] V.Tarokh, N. Sesahdri and A. R. Calderbank, "Space-time codes for high data rate wireless communication: Performance criterion and code construction," *IEEE Transactions on Information Theory*, vol. 44, pp. 744-765, March 1998.

[24] Gerard J. Foschini, "Layerd space-time architecture for wireless communications in a fading environment when using multi-element antennas," *Bell Labs Technical Journal*, 1996.

[25] P. W. Wolniansky, G. J. Foschini, G. D. Golden and R. A. Valenzuela, "V-BLAST : An architecture for realizing very high data rates over the rich-scattering wireless channel," *URSI International Symposium on Signals, Systems and Electronics*, pp. 295-300, 1998.

[26] G. D. Golden , G. J. Foschini, R. A. Valenzuela and P. W. Wolniansky, "Detection algorithm and initial laboratory results using v-blast space-time communication architecture," *IEE Electronic Letters*, vol. 35, no. 1, pp. 14-16, January 1999.

[27] W. Wu and K. Chen, "Linear multiuser detectors for synchronous CDMA communication over rayleigh fading channels," *IEEE International Symposium, Personal, Indoor and Mobile Radio Communications (PIMRC' 96)*, vol. 2, pp. 578-582, October 1996.

[28] G. J. Foschini, G. D. Golden, R. A. Valenzuela and P. W. Wolniansky, "Simplified processing for high spectral efficiency wireless communication employing multi-element arrays," *IEEE Journal on Selected Areas in Communication*, vol. 17, no. 3, pp. 1841-1852, November 1999.

[29] V. Tarok, H. Jafarkhami and A.R. Calderbank, "Space-time block codes from orthogonal designs," *IEEE Transactions on Information Theory*, vol. 45, no. 5, pp. 1456-1467, July 1999.

[30] V. Tarok, H. Jafarkhami and A.R. Calderbank. 1999. "Space-time block codes for wireless communications: performance results," *IEEE Journal on Selected Areas in Communications*, vol. 17, no. 3, pp. 451-460, March 1999.

[31] H. Huang, H. Viswanathan and G. J. Foschini, "Multiple antennas in cellular CDMA systems: Transmission, detection and spectral efficiency," *IEEE Transactions on Wireless Communications*, vol. 1, no. 3, pp. 383-392, July 2002.

[32] S. N. Batalama, M. J. Medley and I. N. Psaromiligkos, "Adaptive robust spread-spectrum receivers," *IEEE Transactions on Communications*, vol. 47, pp. 905-917, June 1999.

[33] U. Mitra and H. V. Poor, "Detection of spread-spectrum signals in a multi-user environment," *IEEE International Conference of Acoustics, Speech, and Signal Processing*, Detroit, MI, vol. 3, pp. 1844-1847, May 1995.

[34] S. Haykin, *Communication systems*, John Wiley and Sons, Singapore, 1994.

[35] S. S. Pillai and M. Harisankar, "Simulated performance of a DS spread spectrum system in impulsive atmospheric noise," *IEEE Transactions Electromagnetic Compat.*, vol. 29, pp. 80-82, 1987.

[36] M. Bouvet and S. C. Schwartz, "Comparison of adaptive and robust receivers for signal detection in ambient underwater noise," *IEEE Transactions Acoustic, Speech, Signal Processing*, vol. 37, pp. 621-626, 1989.

[37] J. Haring and A. J. Vinck, "Coding and signal space diversity for a class of fading and impulsive noise channels," *IEEE Transactions on Information Theory*, vol. 50, pp. 887-895, May 2004.

[38] X. Wang. and H. Vincent Poor, "Robust multiuser detection in non-gaussian channels," *IEEE Transactions Signal Processing*, vol. 47, no. 2, pp. 289-305, February 1999.

[39] D. Middleton, "Statistical-physical models of electromagnetic interference," *IEEE Transactions Electromag. Compat.*, vol. EC-19, pp. 106-127, August 1977.

[40] T.Cihan and G. Ping, "On diversity reception over fading channels with impulsive noise," *IEEE Transactions on Vehicular Technology*, vol. 54, no. 6, pp. 2037-2047, November 2005.

[41] A. D. Spaulding and D. Middleton, "Optimum reception in an impulsive interference environment-Part I: Coherent Detection," *IEEE Transaction Communication*, vol. COM-25, no. 9, pp. 910-923, September 1977.

[42] J. Haring and A. J. H. Vinck, "Performance bounds for optimum and suboptimum reception under class-A impulsive noise," *IEEE Transaction Communication*, vol. 50, no. 7, pp. 1130-1136, July 2002.

[43] P. A. Delaney, "Signal detection in multivariate class-A interference," *IEEE Transaction Communication*, vol. 43, no. 2, pp. 365-373, February 1995.

[44] S. Buzzi, E. Conte and M. Lops, "Optimum detection over Rayleigh fading, dispersive channels, with non-Gaussian noise," *IEEE Transaction Communication*, vol. 45, no. 9, pp. 1061-1069, September 1997.

[45] T. S. Rappaport, *Wireless Communications*, Upper Saddle River, Prentice Hall, 1996.

[46] F. Zheng and S. K. Barton,"Near-far resistant detection of CDMA signals via isolation bit insertion," *IEEE Transactions on Communications*, vol. 43, pp.1313-1317, April 1995.

[47] H. Delic and A. Hocanin, "Performance of robust single-user detection in DS/CDMA systems," *IEEE Wireless Communications and Networking Conference (WCNC 2000)*, vol. 3, pp. 1147-1151, September 2000.

[48] D. Koulakiotis and A. H. Aghvami, "Data detection techniques for DS/CDMA mobile systems: a review," *IEEE Personal Communications*, pp. 24-34, June 2000.

[49] R. Lupas and S. Verdu, "Near-far resistance of multi-user detectors in asynchronous channels," *IEEE Transactions on Communications*, vol. 38, no. 4, pp. 496-508, April 1990.

[50] P. Patel and J. Holtzman, "Analysis of a simple successive interference cancellation scheme in DS/CDMA system," *IEEE Journal on Selected Areas in Communications*, vol. 12, no. 5, pp. 796-807, June 1994.

[51] B. Aazhang and H. V. Poor, "Performance of DS/SSMA communications in impulsive channels-part I: Linear correlation receivers," *IEEE Transactions on Communications*, vol. COM35, pp. 1179-1188, November 1987.

[52] R. Buehrer, "Equal BER performance in linear successive interference cancellation for CDMA systems," *IEEE Transactions on Communications*, vol. 49, no. 7, pp. 1250-1258, July 2001.

[53] Lars K. Rasmussen, Teng J. Lim, and Ann-Louise Johansson, "A Matrix-Algebraic Approach to Successive Interference Cancellation in CDMA," *IEEE Transactions on Communications*, vol. 48, no. 1, pp. 145-151, January 2000.

[54] M. B. Pursley, "Performance evaluation for phase-coded spread-spectrum multiple-access communicationPart I: System analysis," *IEEE Transactions on Communications*, vol. 25, pp. 795-799, August 1977.

[55] D. Middleton and A. D. Spaulding, "Non-Gaussian noise models in signal processing for telecommunications: new methods an results for class A and class B noise models," *IEEE Transactions on Information Theory*, vol. 45, pp. 1129-1149, May 1999.

[56] T. K. Blankenship, D. M. Krizman and T. S. Rappaport,"Measurements and simulation of radio frequency impulsive noise in hospitals and clinics," *In Proceeding of the IEEE Vehicular Technology Conference (VTC 97)*, pp. 1942-1946, 1997.

[57] S. M. Zabin and H. V. Poor, "Efficient estimation of the class A parameters via the EM algorithm," *IEEE Transactions on Information Theory*, vol. 37, pp. 60-72, January 1991.

[58] K. S. Vastola, "Threshold detection in narrowband non-Gaussian noise," *IEEE Transactions on Communications*, vol. COM-32, pp. 134-139, February 1984.

[59] D. Hakan and H. Aykut,"Robust detection in DS-CDMA," *IEEE Transactions on Vehicular Technology*, vol. 51, no. 1, pp. 155-170, January 2002.

[60] D. Liu, Y. Mo and D. Li, "The effect of channel estimation error on MIMO CDMA system," *IEEE Conference on Communications and Networking (Com '06)*, China, vol. Iss, pp. 1-4. October 2006.